CRITICAL REVIEW OF THE REACTIVE ACID TAILINGS ASSESSMENT PROGRAM (RATAP.BMT2)

MEND Project 1.21.1a

April 1990

A RESEARCH REPORT PREPARED UNDER
CONTRACT #28SQ-23440-9-9074

CRITICAL REVIEW OF THE
REACTIVE ACID TAILINGS
ASSESSMENT PROGRAM
(RATAP.BMT2)

Prepared For

CANADA CENTRE FOR MINERAL AND ENERGY TECHNOLOGY
Mineral Sciences Laboratories
555 Booth Street
Ottawa, Ontario
K1A 0G1

by

SENES CONSULTANTS LIMITED
52 West Beaver Creek Road
Unit No. 4
Richmond Hill, Ontario
L4B 1L9

In Association with

BEAK CONSULTANTS LIMITED
14 Abacus Road
Brampton, Ontario
L6T 5B7

April 1990

TABLE OF CONTENTS

EXECUTIVE SUMMARY

Control of acid mine drainage from tailings areas is widely recognized as one of the most serious environmental issues facing many base metal, gold and uranium mine operators today. While collection and treatment of acid mine drainage is commonly practiced at active mine sites, it is generally accepted that continuation of treatment practices for an indefinite period in the post operating phase is neither desirable nor practical. Besides the obvious problems associated with maintaining an effective treatment system after mining activities have ceased, the disposal of chemical treatment plant sludge produced from the neutralization of acid mine drainage is a major operational problem.

Originating from work initiated in the mid-1980's by the Canada Centre for Mineral and Energy Technology, the Reactive Acid Tailings Assessment Program for Base Metal Tailings (RATAP.BMT) was developed as a predictive modelling tool to investigate the factors and processes which control the oxidation of sulfide minerals, to simulate acid generation in mine tailings, to estimate the long-term potential for acid generation in tailings, and to evaluate the effects on acid generation of alternative closeout concepts.

This report describes the extension of the validation of the model by:

1) a discussion of quality assurance procedures followed during each stage of code development and documentation of recent code modifications;

2) a critical review of the concepts behind the program; and

3) a comparative evaluation of computer simulations with a more complete database for the Waite-Amulet zinc/copper mine tailings.

RATAP.BMT addresses questions more numerous and more complex than those addressed by other models. It permits evaluation of the limitations of other modelling work and of many additional questions which are beyond the scope of the other models. However, RATAP.BMT requires a more knowledgeable user and, thus, is more difficult for a novice user to program.

The model considers the following processes:

- sulfide mineral oxidation kinetics as a function of water temperature, oxygen concentration, mass of pyrite, pH, phosphorous concentration, carbon dioxide content, and moisture content.
- oxygen pore-gas diffusivity and its control upon the oxygen flux into the tailings.
- shrinkage of sulfide mineral grains as they oxidize.
- depth-dependent differences in the chemical characteristics of the tailings.
- temperature variation with depth due to oxidation of pyrrhotite, pyrite, chalcopyrite, sphalerite and arsenopyrite.
- moisture variations with depth in the unsaturated zone.
- kinetic reactions between porewater and relevant minerals.
- porewater transport of metals including aluminum, iron, calcium, magnesium, potassium, silica, copper, zinc, and of anions including arsenic, sulfate, and carbonate.

Model validation was based on the comparison of model predictions for selected parameters to data collected on the Waite–Amulet tailings during the Phase 2 and Phase 3 field studies. Part of the data was used to calibrate the site dependent parameter estimates. The second part of the data was used to verify the model both in the temporal and spatial (i.e. with respect to depth) sense. The modelled constituents included temperature, pH, oxygen concentration (variation with depth), and porewater concentration of sulfate, ferrous and ferric iron, dissolved copper, and zinc.

The final test involved running the model both in a deterministic and probabilistic manner. The probabilistic simulations were based on selecting parameter values from established distribution functions. The geometric mean values of the probabilistic outputs were used for comparison to the results of the deterministic runs using nominal parameter values.

SOMMAIRE

L'élimination du drainage minier acide dans les aires d'entreposage des résidus est largement reconnu comme l'une des questions environnementales les plus importantes auxquelles ont actuellement à faire face les exploitants de métaux communs, d'or et d'uranium. Même si le traitement des eaux de drainage acides est de pratique courante sur les sites miniers actifs, il est généralement admis qu'il n'est ni souhaitable ni pratique de poursuivre le traitement des eaux de drainage pendant une période indéfinie après la fin de l'exploitation. En plus des problèmes évidents associés à l'entretien d'un système efficace après la cessation des activités minières, l'élimination des boues d'usines de traitement chimiques, produites par la neutralisation des eaux de drainage acides, constitue un problème opérationnel d'envergure.

Découlant des travaux entrepris au milieu des années 1980 par le Centre canadien de la technologie des minéraux et de l'énergie, le Programme d'évaluation des résidus acides réactifs des métaux communs (PERAR.MC), est un outil de modélisation de prévision mis sur pied pour analyser les facteurs et les procédés qui régissent l'oxydation des minéraux sulfurés, pour simuler la production d'acide dans les résidus miniers, pour évaluer le potentiel à long terme d'acidification des résidus et pour déterminer les effets sur l'acidification des autres concepts de fermeture.

Le présent rapport fait une description de la portée de validation du modèle de la façon suivante :

1) traitement des procédés de contrôle de la qualité au cours de chacune des étapes de la programmation et documentation des récentes modifications de programme;

2) analyse critique des concepts sous-jacents au programme; et

3) évaluation comparative des simulations informatiques avec une base de données plus complète pour les résidus miniers de zinc-cuivre de Waite-Amulet.

Le PERAR.MC traite de questions plus nombreuses et plus complexes que les autres modèles. Il permet d'évaluer les limites d'autres travaux de modélisation et de nombreuses questions supplémentaires qui sont hors de la portée des autres modèles. Cependant le PERAR.MC nécessite davantage de connaissances de la part de l'utilisateur de sorte qu'il est plus difficile à programmer pour le débutant.

Le modèle traite les procédés suivants :

- la cinétique d'oxydation des minéraux sulfurés en fonction de la température de l'eau, de la concentration en oxygène, de la masse de la pyrite, du pH, de la concentration en phosphore, de la teneur en gaz carbonique et en humidité.
- la diffusivité de l'oxygène gazeux interstitiel et son rôle sur le flux d'oxygène pénétrant dans les résidus.
- le retrait des grains de minéraux sulfurés à mesure qu'ils s'oxydent.
- les différences chimiques des résidus en fonction de la profondeur.
- la variation de la température en fonction de la profondeur, causée par l'oxydation de la pyrrhotite, la pyrite, la chalcopyrite, la sphalérite et l'arsénopyrite.
- les variations de l'humidité dans la zone non saturée en fonction de la profondeur.
- les réactions cinétiques entre l'eau interstitielle et les minéraux pertinents.
- le transport dans l'eau interstitielle de métaux (aluminium, fer, calcium, magnésium, potassium, silice, cuivre, zinc) et d'anions (arsénic, sulfate et carbonate).

La validation du modèle a consisté à comparer les prévisions par modèle de certains paramètres avec les données recueillies sur les résidus de Waite–Amulet au cours des phases 2 et 3 des études réalisées sur le terrain. Une partie des données a servi à calibrer les estimations relatives aux paramètres en fonction du site. L'autre partie des données a servi à vérifier le modèle sur les plans temporel et spatial (c'est-à-dire en fonction de la profondeur). Les éléments modélisés ont été la température, le pH, la concentration en oxygène (variation en fonction de la profondeur) et la concentration dans l'eau interstitielle du sulfate, du fer ferreux et ferrique, du cuivre dissous et du zinc.

L'essai final a consisté à exploiter le modèle d'une façon déterministe et probabiliste. Les simulations probabilistes étaient basées sur le choix des paramètres à partir des fonctions de distribution établies. Les valeurs moyennes géométriques des données de sortie probabilistes ont été utilisées pour comparer les résultats des traitements déterministes en utilisant les valeurs nominales des paramètres.

1.0   INTRODUCTION

1.1   Background

Control of acid mine drainage from tailings areas is widely recognized as one of the most serious environmental issues facing many base metal, gold and uranium mine operators today. While collection and treatment of acid mine drainage is commonly practiced at active mine sites, it is generally accepted that continuation of treatment practices for an indefinite period in the post operating phase is neither desirable nor practical. Besides the obvious problems associated with maintaining an effective treatment system after mining activities have ceased, the disposal of chemical treatment plant sludge produced from the neutralization of acid mine drainage is a major operational problem.

Recognizing the seriousness of this problem, the Canada Centre for Mineral and Energy Technology, initiated work in the mid 1980's into investigating the factors and processes which control the oxidation of sulfide minerals and on developing a predictive modelling tool to simulate acid generation in mine tailings. The primary objective of this work was to provide a model for predicting the long-term potential of acid generation in tailings and for evaluating the effects on acid generation of alternative closeout concepts.

The first of these studies was completed in 1984 by SENES Consultants Limited on behalf of the National Uranium Tailings Program. This study documented the role that bacteria play in the oxidation of pyrite and other sulfide minerals in uranium mine tailings (SENES, 1984). The mechanisms involved in iron and sulfur oxidation were detailed as were the kinetic relationships reported in the literature for the bacterial oxidation and chemical oxidation of sulfide minerals.

In 1986, SENES Consultants Limited and Beak Consultants Limited developed the Reactive Acid Tailings Program (RATAP) for the National Uranium Tailings Program. The RATAP model was developed to provide an estimate of the upper and lower limits of the rate and quantity of acid generation by the bacteria-assisted oxidation of pyrite present in uranium mine tailings (SENES and Beak, 1986).

SENES and Beak adapted the RATAP model to base metal tailings, as part of a project sponsored by CANMET, in 1988. The model developed, the Reactive Acid Tailings Assessment Program for Base Metal Tailings, Version 1 (RATAP.BMT1), also provided an estimate of the upper and lower limits of acid generation by the bacteria-assisted oxidation of sulfides. The sulfides modelled included pyrite, pyrrhotite, chalcopyrite and sphalerite. In addition, it calculated the aqueous concentrations of zinc and copper.

In 1989, SENES and Beak extended RATAP. BMT1 to allow for arsenic-bearing components in the tailings. Version 2 (RATAP.BMT2) incorporates an algorithm for arsenic geochemistry to accommodate an additional sulfide, arsenopyrite, and to facilitate the calculation of aqueous concentrations of arsenic (SENES and Beak, 1989).

Since its original conception, the model has undergone several conceptual modifications and has been calibrated and validated extensively on pyritic uranium tailings. Partial validation of the modified computer model (i.e. RATAP. BMT2) was also performed in previous work using the Phase 2 field study data on the high sulfide tailings at Waite-Amulet in northeastern Quebec, some relevant data from pyritic uranium tailings investigations in the Elliot Lake area of northern Ontario, and laboratory observations. Due to incomplete data, these validation efforts were only partially successful, since the available database did not allow comparison of predicted and measured values for a full range of parameters. Furthermore, the validity of the geochemical concepts used could not be fully assessed.

1.2   Model Application

RATAP.BMT is both a powerful analytical tool and an effective planning aid. Used analytically, the model predicts concentrations for several solid, aqueous and gaseous phase constituents to enable the assessment of the rate and quantity of acid generation in pyritic tailings. During planning, RATAP.BMT allows an evaluation of the benefits of short and long-term tailings management options and facilitates the development of alternative reclamation or closeout strategies.

As a test of the RATAP model, predictions of acid generation in the Nordic tailings were made for a timeframe spanning the period from 1969 to 2041. Analysis of the data indicated that approximately 90,000 tonnes of acid have been produced at the Nordic site to date. Of this

amount, it is estimated that 25% has been neutralized at the lime treatment plant, 45% remains in storage in the tailings porewater and sand aquifer underlying the site, and 30% has been neutralized by the buffering capacity of the tailings and sand aquifer. As of 1988, the rate of acid being generated was approaching the rate of acid release from the system. Although the rate of acid production is declining and currently is at about one-half the rate predicted for the early 1970's, acid generation will continue well into the 21st century because of the large inventory of pyrite remaining to be oxidized.

The RATAP model has also been applied on several of the tailings areas at Elliot Lake to evaluate the potential benefits of closeout options in reducing acid generation. One concept which has been discussed on numerous occasions involves the application of a cover of earthen material or depyritized tailings. For this evaluation, it was assumed that the cover material (soil or depyritized tailings) had the same physical characteristics as tailings. The results demonstrated that cover application will reduce the acid generation rate substantially but does not necessarily impact upon the total quantity of acid generated unless the cover application results in a rise in the water table within the basin.

Application of RATAP to the Elliot Lake situation provided a basis for assessing the need for remedial measures at non-operating properties, for assessing the extent and duration of acid generation and the long-term need for treatment, and most importantly, for comparing the environmental and cost effectiveness of remedial measures and reclamation proposals.

1.3   Study Objectives and Approach

This report describes the extension of the validation of the RATAP.BMT2 computer program by:

1)   a discussion of quality assurance procedures followed during each stage of code development and documentation of recent code modifications;

2)   a critical review of the concepts behind the program; and

3)   a comparative evaluation of computer simulations with a more complete database for the Waite-Amulet zinc/copper mine tailings.

1-3

2.0 CRITICAL REVIEW OF THE CONCEPTS

2.1 Acid Mine Drainage Modelling

The development of a model to answer questions concerning acidic drainage from mine tailings is dependent upon the objectives of the investigator. Different questions asked about the same tailings system will necessitate the use of different models. The background of the professional using the models will also influence the selection of a model. These models have the following objectives:

1) to provide a useful predictive basis for making decisions concerning tailings management alternatives; and/or

2) to describe mathematically the most important interactions involving chemical interactions and migrating ground water.

A model is an abstraction of reality that describes, in either qualitative or quantitative terms, a certain set of the complex interrelationships of the system being studied. A quantitative model is described herein as being either empirical or deterministic. An empirical quantitative model involves a statistical relationship between two or more variables. A deterministic quantitative model is based upon physico-chemical principles such as the law of conservation of mass.

In any given situation, the costs of management procedures to ameliorate environmental impacts can be determined with relative ease and accuracy. However, the results or benefits of such procedures can only be predicted with assurance if quantitative models, capable of predicting the response of the tailings to a given management strategy, are available.

The utility of such models for assessing the effects of tailings management alternatives on acidic fluxes is determined by the degree to which the models adequately abstract the coupled nature of hydrogeology and chemistry and are readily understood and applied in a particular use.

A variety of frameworks have been presented in the literature for evaluating the utility of a model, its capabilities and limitations.

2-1

Various investigators have presented their approach to the modelling process (e.g., Orlob, 1975). We find it most useful to use the following seven steps:

1)   problem definition and objective formulation,

2)   system abstraction and discretization (conceptual model, physical and chemical boxes),

3)   model construction,

4)   mathematical solution,

5)   model calibration,

6)   model validation, and

7)   model prediction.

A model is constructed to fulfill certain objectives. Different objectives necessitate different spatial and temporal scales. For example, one's objective may be to develop a model capable of predicting how long into the future acidic fluxes from a tailings pile will be a problem. Alternatively, one's objectives may be to predict the seasonal change in pH in tailings porewater at a specific depth in the tailings pile. The former objective involves a time scale of years to decades while the latter involves a time scale of weeks or months. The spatial scale of the former objective is the thickness of the tailings mass while the spatial scale of the latter objective is 1 m or less. If one is particularly concerned with predicting the pH variation at the oxidation front, the spatial scale may be 0.01 to 0.1 m.

These examples illustrate particular points about the terminology: spatial scale, temporal scale. These "scales" represent the size of the "time block" or the "distance block" over which significant changes occur. They also become the size of the "time block" or of the "size block" (spatial scale) which is used for organizing the model.

System abstraction and discretization is the physical, biological and chemical representation of the tailings deposit. The system boundaries are selected based on field data which describe the physical, biological and chemical characteristics of the system and from data which describe the flows of mass or energy into and out of the system. Selection of the system boundaries is made to be consistent with the model objectives. A box (e.g., a layer of the unsaturated zone) is considered as one of a spatially distributed set of entities each of which has the capacity to store mass or energy; the total number of boxes describes the physical structure of the entire system.

A box is chosen such that flows of mass or energy occur between interconnected boxes, but such

that spatial variations of mass or energy within the box are small. Thus, the tailings mass is divided into volumes (boxes) which are each sufficiently homogeneous such that physical, chemical or biological detail necessary for the realization of a model's objectives is not lost. In the RATAP model, the boxes consist of a number of layers, one lying above the other; for example, for 20 layers in the unsaturated zone and 2 layers in the saturated zone, the total number of boxes is 22.

A box is subdivided into compartments, each describing a different biological or chemical entity deemed to be important to fulfill the model's objective(s). Thus, each compartment describes a different form of mass or energy found within a box (e.g., iron concentration in the porewater, goethite or pyrite content of tailings solids, temperature, and oxygen content of air), and all the compartments within a box describe all of the forms of mass or energy stored within that box. Physical, biological and chemical flows of mass or energy may occur between interconnected compartments.

As Okubo (1971) notes, "the box model treats mixing "averaged" over each box and attempts to see changes only as between boxes. The mixing processes at the interfaces of the boxes are parametrically disguised as exchange - or transfer-rate constants with the dimensions of (t^{-1})." Okubo also notes that other investigators have found the well-mixed assumption unnecessary for successful box model application, and have related the box transfer-rate coefficients to advective and eddy diffusivity processes described in 1-D and 2-D transport models.

Construction of a model involves four basic steps:

1) identifying the physical, biological and chemical processes and the corresponding laws governing the rates of mass flow between compartments and/or boxes (e.g., pyrite oxidation, oxygen diffusion; gypsum precipitation or dissolution);

2) listing the assumptions made, including simplifications of physical laws;

3) constructing systems of mathematical equations which describe the behaviour of the system. The system of equations is constructed by writing a statement of conservation of momentum, energy or mass for each compartment in each box. For example, the rate of change of mass equals the difference between the rate of mass input and the rate of mass output; and

4)   evaluating the boundary conditions.

The mathematical solution involves using an analytical solution or numerical solution for the system of equations to obtain the predictions made by the model. If computer techniques are used, the mathematical solution also involves code verification. Code verification is the process used to show that the mathematical equations have been properly coded in the computer language.

Model calibration consists of selecting a set of coefficient values from field measurements and/or literature values such that the model output duplicates a set of *in situ* measurements of some known system. The coefficients are constants describing empirical relations where fundamental laws are unavailable. Their uniqueness is partially a function of the spatial and temporal structure of the model. Selection of values for coefficients for which field measurements have not been made is usually done by varying the coefficient values over the range of reported literature values until satisfactory agreement is reached between model predictions and environmental observations. Coefficient values obtained from field measurements may also be varied if the modeler decides that a measurement does not describe conditions throughout a compartment. Alternatively coefficient values may be determined using an optimization method which minimizes the difference between model predictions and observations.

Model validation is discussed in Section 3.1.

Other models reported in the literature include those of the Rogowski group (e.g., Jaynes *et al.*, 1984a, b) and of the Ritchie group (e.g., Davis and Ritchie, 1986; Davis *et al.*, 1986). The questions addressed by RATAP.BMT have been defined and coded independently of these other modelling efforts. This has resulted in some similarities and some significant differences between the various modelling efforts.

2.1.1   Jaynes *et al.* Modelling Approach

Jaynes *et al.* (1984a, b) evaluated acidity fluxes from spoils associated with coal strip mines. Pyrite dynamics are based upon the total time required to oxidize all pyrite within a box in the discretized vertical profiles (one-dimensional).

2-4

"The rate of pyrite oxidation is assumed to be controlled by both first-order reaction kinetics and the combined diffusion rates of the products and reactants to the reaction site within shale blocks. Both oxygen and ferric iron may serve as the oxidant. Ferric iron concentrations are controlled by iron complexation and precipitation reactions that are assumed to be rapid and completely reversible. Ferric iron is assumed to be produced by both direct chemical oxidation of ferrous iron and oxidation of ferrous iron by autotrophic bacteria. Environmental factors which affect the bacterial "activity" are oxygen concentration, temperature, and solution pH. Fluctuations in the bacterial "activity" caused by changes in their environment are considered to be rapid so that their "activity" is always at its maximum. Pyrite oxidation and bacterial "activity" are linked through their modification of a shared environment."

"Oxygen is the ultimate electron acceptor for pyrite oxidation and is considered to be supplied to the profile by gaseous diffusion, from the surface first through the large pore spaces between the shale blocks then into the blocks to reach the reactive pyrite surfaces. Diffusion of oxygen in the blocks is implicit in the model. Sources for hydrogen ion include pyrite oxidation, iron complexation and precipitation reactions. Sinks for hydrogen ion include ferrous iron oxidation, hydrolysis of the rock matrix, and exchange reactions. These last two sink reactions are lumped together as one reaction in the model and given a pH dependence in the form of a simple empirical reaction. Carbonate neutralization reactions are not considered explicitly at this time. Hydrogen ion, ferrous and ferric iron and ferric complexes, sulfate and bisulfate, and solution "acidity" are leached from the spill profile by a constant water flux."

The major differences between the model of Jaynes *et al.* (1984) work and RATAP.BMT include the following concepts considered by RATAP:

- acid flux based on particle size distribution;
- mechanistic (rather than empirical) modelling approach;
- carbonate mineral interactions;
- mass balance on the various mineral phases;
- explicit inclusion of all relevant porewater cations and anions and use of the electroneutrality equation to calculate pH, rather than use of an empirical relationship of Jaynes *et al.* for calculating pH; and
- uncertainty analyses.

Jaynes *et al.* (1984) found that the oxidation of pyrite is primarily controlled by the oxygen

diffusion rate. There is no evidence of kinetic control for any substantial period.

According to the RATAP model, the acidic flux depends on both the kinetics and oxygen transport. As time progresses, a quasi-steady state in oxidation is reached and the thickness of the oxidizing zone remains essentially constant. As the sulfide minerals are exhausted from the zones near the surface, diffusion control becomes more important and the RATAP concept becomes essentially identical with those employed by Jaynes *et al.* (1984).

2.1.2   Ritchie *et al.* Modelling Approach

The work of Ritchie's group is a landmark in the sulfidic mine waste literature which parallels the development of RATAP.

Their main objective was to calculate the acidic flux from tailings.   They assume that the "oxidation rate is limited by the rate that oxygen is supplied to oxidation sites within the particles comprising the wastes. Oxygen supply is assumed to be controlled by diffusion through the pore space of the wastes followed by diffusion into a moving reaction front within the particles. An approximation is made which incorporates the effect of reaction of pyrite into the boundary conditions. A further approximation involving a pseudo steady-state simplification is made that allows an analytical solution to be formulated." The results predicted by this analytical solution are compared with the calculations of an earlier simpler model (Harries & Ritchie, 1983). The chemistry of the porewater is ignored.

In further work, two additional refinements were considered. "In the first, the limiting approximations were examined by developing a numerical solution to the set of equations for oxidation in pyrite mine wastes under natural conditions. The numerical solution allows one to examine oxidation at the moving front within the blocks comprising the wastes. Properties predicted by the numerical solution were compared with results predicted by an approximate analytical solution."

In the second refinement, "the assumption of just one initial size for pyritic blocks was relaxed to take proper account of the range of particle sizes in the wastes. Comparison of the simpler model with the more realistic model (i.e., incorporating the sulfide mineral) shows that for practical purposes the simpler model is good enough to assess the magnitude and longevity of the environmental impact of pollutant generation in the wastes. It is, however, essential to

include the particle size distribution to obtain accurate estimates of the heat source distribution profile and to a lesser extent the oxygen concentration profile, two parameters that can be measured and used to assess the applicability of the model to the real field situation."

In an extension of this work (Bennett *et al.*, 1989) the convection and diffusion of oxygen into heaps was examined. "Both downward oxygen transport through the surface and horizontal movement in through the side were modelled. Measured values of pyrite oxidation were used to evaluate kinetics. The results show that for time scales smaller than about two years, diffusion is always an important oxygen supply process. For air permeabilities less than about 10^{-10} m^2 thermal convection is never a significant air transport mechanism at these early times but it is significant at permeabilities exceeding 10^{-10} m^2. For time scales longer than 2 years after establishing the heap, and at permeabilities less than about 10^{-10} m^2, thermal convection can become significant depending on the magnitude of other parameters such as heap size and pyrite content."

Similar to the findings of RATAP, oxygen diffusion is a dominant process controlling pyrite oxidation. However, their formalism does not allow one to assess the relative importance of kinetics versus diffusion upon controlling oxygen fluxes into the heap as readily as RATAP.

An overview of the different components addressed by each of these models is summarized in Table 2.1. In general, the models from the left column to the right most column represent a gradation from those which were developed to answer simple questions to those which were constructed to address more complex questions.

In terms of deciding whether a more complex model is required, the work of Ritchie's group indicates that for some questions, more complicated treatments (e.g., considering the particle size distribution of sulfide mineral blocks) do not give significantly different answers than simpler treatments (e.g., uniform sized pyrite minerals). However, a systematic evaluation of all possible simplifications is required before one can decide that a particular degree of detail is <u>not</u> required in a model.

To assist the MENDS committee in their evaluation of models, a systematic listing of simplifications for RATAP could be made. Then a comparison of RATAP's calculations with and without these simplifications could be made to determine whether particular modifications/simplifications are required for the model.

2-7

Table 2.1

COMPARISON OF CAPABILITIES OF SEVERAL MODELS

Component	Jaynes _et al._	Harries & Ritchie	Nicholson _et al.,_ 1986	RATAP.BMT2
Sulfide Mineralization	Pyrite in shale blocks	Sulfide in blocks of rock	Pyrite particles	Pyrite, pyrrhotite, chalcopyrite, sphalerite and arsenopyrite particles
Sulfide Particle Size Distribution	No	No/Yes	No	Yes
Sulfide Mineral Oxidation Kinetics	Biological, chemical	Implicit as boundary condition	First order coefficient	Biological, chemical
Diffusion Coefficient/ Oxygen Transport	Constant inter-particle and through porous media	Constant inter-particle and through water in porous rock	Calculated from moisture content	Calculated from moisture content
Pore Water Chemistry	Yes	No	No	Yes
Neutralization	Semi-empirical	-	-	Thermodynamic/ kinetic
Mass Balance on Sulfide	Yes	Yes	Yes	Yes
Mass Balance Other Minerals	No	No	No	Yes
Effectiveness of Management Options	-	-	-	Yes
Uncertainty Analysis	No	No	No	Yes

Using the work of Ritchie's group and the RATAP.BMT as a base, the following summary can be made.

The work of Ritchie's group present an oxygen transport-control approach to model construction and testing. It involves defining the problem, assessing important mechanisms, and then making the appropriate modelling assumptions upon which the code formalism and model predictions are based. As even more questions are raised about the modelling assumptions, more complex models must be formulated to address these questions concerning the appropriateness of the original model. In the case of the more complex questions, Ritchie's work indicates that the original models were essentially "good enough" for the relatively simple questions being asked, but that the models required significant modification when the questions being asked, changed.

In reflection of questions addressed by the RATAP.BMT code, it addresses a larger number of questions and questions which are more complex than those addressed either by the work of Ritchie's group or by Jaynes' work. It permits evaluation of the limitations of the modelling work of these two respective investigators. RATAP.BMT permits evaluation of many additional questions which are beyond the scope of the questions evaluated by these investigators. But RATAP.BMT requires a more informed user and is harder for a novice user to obtain an understanding of the main processes controlling acidification reactions and the resultant transport of metals and anions.

2.1.3   The RATAP.BMT2 Modelling Approach

RATAP.BMT and RATAP.BMT2 were formulated to answer the following questions:

1.   How much time is required to oxidize all pyrite in a tailings area?

2.   How long will acid generation be a problem for a tailings area?

Or, more specifically:

i)   How much time is required to oxidize most of the sulfide minerals in the unsaturated zone? (This is similar to question 1 above.)

ii)   How much time is required before the acid generation flux decreases by one order of

magnitude or two orders of magnitude to cause a substantially different geochemical regime than at present? For this interpretation, the same variables used for question 1 would be required.

iii)   How much time is required before the acid flux reaches a specific level (e.g., x mol acid.m^{-2}.y^{-1}) which the environment can accept? (This question is addressed below under question 3.)

3.   What is the acid flux from a tailings area?

4.   What is the flux of acidity and toxic heavy metals from a tailings area?

5.   What is the uncertainty in estimates of fluxes of acidity and metals from a tailings area?

The model considers the following processes:

- sulfide mineral oxidation kinetics as a function of water temperature, oxygen concentration, mass of pyrite, pH, phosphorous concentration, carbon dioxide content, and moisture content.
- oxygen pore-gas diffusivity and its control upon the oxygen flux into the tailings.
- shrinkage of sulfide mineral grains as they oxidize.
- depth-dependent differences in the chemical characteristics of the tailings.
- temperature variations with depth due to oxidation of pyrrhotite, pyrite, chalcopyrite, sphalerite and arsenopyrite.
- moisture variations with depth in the unsaturated zone.
- kinetic reactions between porewater and relevant minerals.
- porewater transport of metals including aluminum, iron, calcium, magnesium, potassium, silica, copper, zinc, and of anions including arsenic, sulfate, and carbonate.

The concepts adopted for modelling a tailings area are illustrated on Figure 2.1. The tailings soil profile is subdivided into the unsaturated zone, capillary fringe and saturated zone. Conditions conducive to the oxidation of sulfide minerals are limited to the unsaturated zone and top layer of the capillary fringe due to the barrier posed by water to oxygen transport. Hence, the characteristics of the tailings mass in the top horizon may be subdivided into twenty layers with each layer having its own distinct physical and chemical properties. In contrast, the saturated

FIGURE 2.1

CONCEPT ADOPTED
FOR MODELLING OF TAILINGS
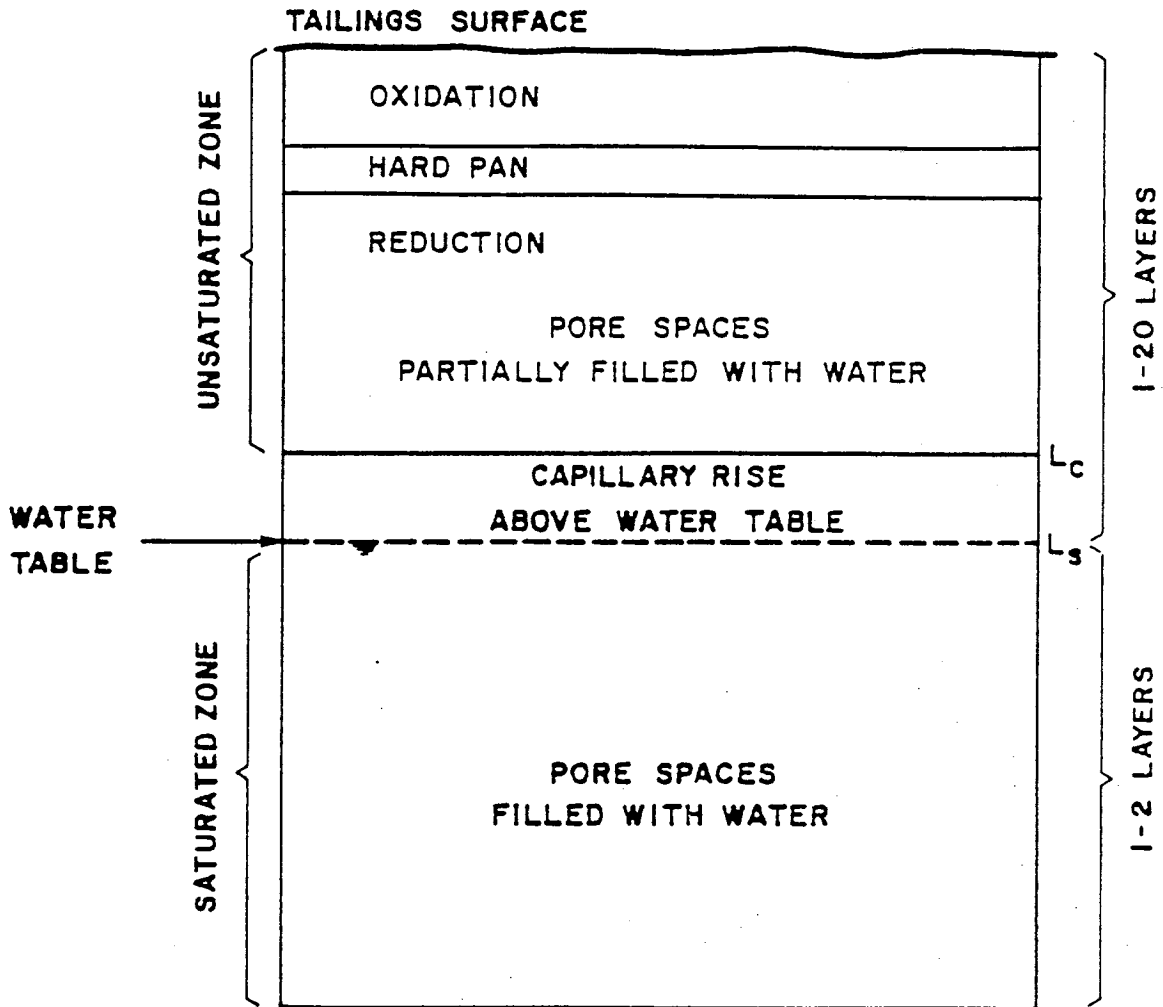
zone, which is a reducing environment, is modelled as either a one or two layer system depending on the flowpath assumed for the tailings porewater.

Precipitation entering the tailings is modelled to flow downward through the unsaturated zone and capillary fringe. On entering the saturated zone, a portion of the flow may be modelled as moving horizontally through the tailings mass and emerge as seepage passing through or beneath the perimeter dams while the remaining portion moves further downward into a subsurface aquifer beneath the tailings.

The rate and quantity of acid generated from the biochemical oxidation of sulfide minerals is dependent on a host of factors which have been extensively reported in the literature and were reviewed in an earlier report by SENES (1984). The RATAP.BMT2 code accounts for many of these factors and is based upon principles of mass balance, geochemical kinetics or equilibria, where appropriate, and solution transport to estimate the pH and the acidity of tailings porewater. The geochemical and biochemical formulations currently used in RATAP.BMT2 include three types of modelling expressions: a) dynamic expressions; b) equilibrium expressions; and c) empirical expressions.

Dynamic expressions are used for modelling time dependent processes. These include sulfide oxidation kinetics, mass transport (oxygen, water, chemical constituents) and energy (enthalpy) transport. The dynamic processes are evaluated for each tailings layer. Although the calculation procedure allows steady state approximation each month, the time dependence of these processes is an important feature of the model.

Equilibrium concepts are used in RATAP.BMT2 for modelling solid dissolution, aqueous speciation, ionic balance (neutralization/buffering), ion exchange, and adsorption processes. It is assumed that these reactions, although dynamic in nature, are sufficiently fast, so that the time scale may be neglected (i.e. processes are essentially instantaneous).

Empirical expressions are used to model periodic (seasonal) variations of temperature, and atmospheric precipitation. These natural processes are modelled by empirical expressions, which have no apparent physical significance (other than built-in periodicity).

In this section of the report, the concepts and theories incorporated into the RATAP.BMT2 code are critically reviewed to assess whether they are appropriate for the potential applications for

2-10

which RATAP.BMT2 may be used, whether they need to be revised in light of current knowledge or whether they need to be expanded to include other factors or processes not included in the current version. Finally, the user-friendliness of the model and its potential use by the mining community are discussed.

2.2   Conceptual Considerations

2.2.1   Hydrogeology

Flow through a tailings pile is modelled in a very simplistic and straight forward manner. Precipitation landing on the tailings watershed is partitioned into a component which flows across and around the tailings area as surface flow and a residual component which penetrates the tailings and moves downward to the saturated zone. Tailings porewater entering the saturated zone is further partitioned into a component which moves horizontally through the tailings to emerge as seepage at the perimeter dams and a component which moves vertically downwind to join a deep subsurface aquifer.

To run the model, the user must specify the monthly infiltration rate, the fractional split in the flow between the horizontal and vertical flowpaths as well as the depth to the water table (i.e. phreatic surface). The user is then required to have a prior understanding of the hydrologic and hydrogeologic characteristics of the tailings area and the effects that closeout or reclamation options would have on these characteristics. An obvious question which may be posed here is: should the RATAP.BMT2 code include detailed hydrologic and hydrogeologic models? If so, what form should they take?

Given the structure of the RATAP.BMT2 model, we believe it would be unwise to incorporate detailed surface and ground water flow models into the code for several reasons. Firstly, analysis of flow conditions in a tailings area can be carried out independently, for the most part, of the evaluation of acid generation. Hence the analysis of depth to the water table, flowpaths and flow rates can be undertaken for any number of conceivable closeout options prior to selecting those options which offer most promise for full analysis. Once the hydrogeology of a tailings area is understood, the results can be adequately simplified for input into RATAP.BMT2.

Secondly, the expertise required to understand and run a hydrogeological model is quite

different from that required to understand and run a biogeochemical model such as RATAP.BMT2. Consequently it will generally be necessary to involve at least two team members with appropriate expertise in the investigation.

Thirdly, the RATAP.BMT2 model treats a tailings area as a multi-layer system in contrast to the continuous three dimensional hydrogeologic models. The dimensions of the layers are fixed at the start of each run using RATAP.BMT2 to permit the mass inventory of sulfide minerals and chemical precipitates to be tracked with time. Also, the water table is set at a constant depth over the area being modelled. In reality, the depth to the water table will vary considerably across a tailings area as will the physical and chemical characteristics of the tailings. In applying the RATAP or RATAP.BMT2 models, it will often be desirable to subdivide a tailings area into several segments each of which has its own characteristics. Acid generation in each sub-area can then be assessed independently and aggregated to determine the overall total acid production for the entire area with time. This approach has been successfully applied to the Nordic tailings area in Elliot Lake, Ontario using the RATAP model.

2.2.2   Steady State Versus Non-Steady State

An implicit concept in the development of the RATAP models has been the assumption of steady state. This assumption was uniformly applied for each process. There were both theoretical and computational reasons underlying this concept. First, the key transport processes (for example, the diffusion of oxygen in the gaseous pore space) were shown to be significantly faster than the monthly time frame. On the other hand, the kinetic geochemical processes (pyrite oxidation) were significantly slower. Consequently, the system would either remain in the vicinity of or rapidly approach a steady state condition. It should be emphasized that the steady state approximations were performed on a monthly basis. The net effect of this monthly approach to steady state was a response profile that resembled a dynamic response.

A major advantage of the steady state approach is computational. The differential equations for a time-dependent system become algebraic relationships using steady state assumptions. These sets of algebraic equations are readily solved by standard, matrix based algorithms. On the other hand, the non-linear differential equations require numerical integration, which greatly diminishes the speed of the program.

The differences between the steady state approach and the unsteady state solution may be

illustrated by the following simple example. Let us consider the following differential equation:

$$\frac{dy}{dt} = R(t) - \left(\frac{1}{\tau}\right) y \qquad\qquad (2.2.2\text{-}1)$$

where:

y	=	dependent variable
t	=	time
τ	=	first order time constant
$R(t)$	=	time dependent rate

Discretizing the equation in monthly time steps results in the analytical solution illustrated in Table 2.2a. These calculations illustrate that both the overall trend and the mean values of the dependent variable are similar when calculated by the two methods. However, these calculations reflect a highly simplified situation and the validity of the steady state assumptions requires more extensive testing.

2.2.3   Constant Versus Variable Layer Depth

The dynamic events in RATAP were modelled by numerical methods based on finite differences and a "box" approach. The finite difference method (with forward differencing) was used to solve second order differential equations involving gaseous oxygen and energy (heat) transport through the tailings. Solute and liquid transport modelling was based on a numerical technique known as Thomann's controlled volume approach. Although this technique was originally used for modelling estuarine environments, it has been proven to be useful for many other situations. The tailings are treated as a series of segments extending from the surface to the hydraulically saturated zone. Conditions and porewater quality within each zone are assumed to be homogeneous and well-mixed. These assumptions within a segment do not preclude variability from one segment to another.

The application of the controlled volume approach to a modelled constituent in the tailings pore space results in the following differential equations:

2-13

TABLE 2.2a

COMPARISON OF STEADY STATE AND
UNSTEADY STATE SOLUTIONS

Month	R(t)	Steady State Value	Unsteady State Value
1	1.59	1.59	1.44
2	5.00	5.00	3.69
3	7.07	7.07	5.83
4	8.66	8.66	7.62
5	9.66	9.66	8.91
6	10.00	10.00	9.60
7	9.66	9.66	9.64
8	8.66	8.66	9.02
9	7.07	7.07	7.79
10	5.00	5.00	6.03
11	1.59	1.59	3.22
12	0.00	0.00	1.18
Annual Mean		7.16	6.16

$$\frac{dC_i}{dt} = \frac{\Sigma \alpha_i R_i}{\epsilon_i} + \left(\frac{F_{i-1}}{\epsilon_i V_i}\right) C_{i-1} - \left(\frac{F_i}{\epsilon_i V_i}\right) C_i + \left(\frac{D_{e,i}}{\epsilon_i \bar{Z}^2_{i-1}}\right)(C_{i-1} - C_i)$$

$$+ \left(\frac{D_{e,i}}{\epsilon_i \bar{Z}^2_{i+1}}\right)(C_{i+1} - C_i) \qquad \text{if } C_i < C_{eq}$$

$$W_i = \Sigma \alpha_i R_i + \left(\frac{F_{i-1}}{V_i}\right) C_{i-1} - \left(\frac{F_i}{V_i}\right) C_{eq} + \left(\frac{D_{e,i}}{\bar{Z}^2_{i-1}}\right)(C_{i-1} - C_{eq})$$

$$+ \left(\frac{D_{e,i}}{\bar{Z}^2_{i+1}}\right)(C_{i+1} - C_i) \qquad \text{if } C_i = C_{eq} \qquad (2.2.3\text{-}1)$$

where:

C_i = concentration of constituent "i" in the pore pace

C_{eq} = equilibrium concentration of constituent "i" in the pore space

V_i = volume of tailings segment "i"

F_i = convective flow from tailings segment "i"

R_i = reaction rate/unit surface area in segment "i"

$D_{e,i}$ = effective diffusion coefficient in segment "i"

$\bar{Z}_{i-1}$ = distances between the midpoint of segment "i" and the midpoint of adjacent segment "i-1"

W_i = rate of deposition of precipitating constituent per unit segment volume

α_i = reactive surface area per segment volume

ϵ_i = porosity (gas filled or liquid filled) of segment "i"

Equation (2.2.3-1) contains advection, diffusion, and reaction terms. Usually, it is further simplified by considering the individual terms. For example, the advective terms are negligible

2-14

(F_i=0) in the case of gaseous oxygen transport, while the diffusive terms are neglected (D_e=0) in the case of liquid phase transport of dissolved ionic species.

The use of the controlled volume approach under steady state conditions has several advantages. The dimensions of the segment need not be uniform and this approach is very useful when variable sized segments are needed. In addition, the steady-state response matrix can be obtained with relative ease and the effect of changes in parameters can be easily studied. The current version of the RATAP model is one dimensional. However, the periodic steady state approach allows expansion to multi-dimensional configuration.

An important aspect of the numerical solution is computational stability. Divergence, often called numerical diffusion, results when step sizes are selected improperly.

The computational stability is more likely to be affected by step size in the case of dynamic (time dependent) calculations. Thomann (1972) has shown that the following inequality constraint is applicable:

$$1 + \frac{u}{Z_i} \Delta t (\beta - \tau) - \frac{2 D_e \Delta t}{Z_i^2} > 0 \qquad (2.2.3-2)$$

where:

$$\beta = \frac{Z_i}{Z_{i-1} + Z_i} \qquad \tau = \frac{Z_{i-1}}{Z_i + Z_{i-1}} \qquad (2.2.3-3)$$

Although the use of unequal tailings depths does not necessarily result in computational chaos, since sufficiently small time steps (Δt) will assure stability, it should be noted that for equal tailings depths, the inequality expression reduces to the following:

$$\frac{2 D_e \Delta t}{Z^2} < 1 \qquad (2.2.3-4)$$

The above inequality is always met when advective flow dominates ($D_e = 0$) and can be

2-15

achieved for any other situation. In addition, the controlled volume based computational procedure can be compared with finite difference methods if equal tailings depth is used. For these reasons, there is an advantage for using equal tailings depths in case of dynamic adaptations of the current RATAP code.

The choice of using unequal versus equal depth sizes is somewhat subjective. The use of small step sizes in the unsaturated zone details the chemical events and provides a sharper focus on the oxidizing front (i.e. oxygen profile). However, uneven step size may lead to computational instability by the inadvertent use of large time steps with small depth steps.

In Table 2.2b, model predictions using constant and variable layer depths are compared. The comparison is performed at a total depth of 1.5 m in the tailings. Although most predictions are comparable, significant differences exist. The differences are most likely due to the unequal residence times arising from the variable depth segments. This can give rise to a "chromatographic effect" of having a high concentration front moving through the system. Recalling that the model calculates the spatial average in a segment, it may be argued that constant segment size is preferable. In the final analysis, the size of the segments should be a compromise between the degree of resolution of the tailings chemistry and computational stability.

2.3   Model Algorithm Development

2.3.1 Temperature

The function of this module is the estimation of temperature with depth in reactive tailings. The first version of the algorithm was part of the RATAP.BMT code. This original version did not work satisfactorily. The TEMP module was completely rewritten and was implemented in RATAP.BMT2 code issued in June 1989. The ensuing section describes a revised, improved version of the RATAP.BMT2 temperature estimation program.

Tailings Temperature Algorithm Development

The calculation of tailings temperature is based on an enthalpy balance. This balance can be expressed by the following partial differential equation:

TABLE 2.2b

COMPARISON OF CONSTANT AND VARIABLE LAYER DEPTHS
ON MODEL PREDICTIONS (DEPTH = 1.5 m)

Constituent	Month = 1		Month = 22		Month = 120	
	Con	Var	Con	Var	Con	Var
Copper (mg/L)	0.07	0.11	0.01	0.39	0.46	2.1
Aluminum, total (mg/L)	0.11	0.11	0.11	0.11	0.11	23.2
Iron (III), total, (mg/L)	0	0	0.31	0.7	0.13	1.9

Con = Constant Layer Depths
Var = Variable Layer Depths

$$\rho C_p \frac{\delta T}{\delta t} = Q + k \frac{\delta^2 T}{\delta Z^2} + F_w C_w \frac{\delta T}{\delta Z} + \Delta H_{vap} \quad E_w \qquad (2.3.1\text{-}1)$$

where

ρ = density of the tailings ($kg.m^{-3}$)

C_p = heat capacity of the tailings solids ($J.kg^{-1}$)

Q = internal enthalpy generation ($J.m^{-3}.s^{-1}$)

k = thermal conductivity ($J.m^{-1}.s^{-1}K^{-1}$)

F_w = water flux ($mol.m^{-2}s^{-1}$)

C_w = heat capacity of water ($J.mol^{-1}$)

ΔH_{vap} = enthalpy of evaporation ($J.mol^{-1}$)

E_w = evaporative water loss ($mol.m^{-3}$)

T = temperature (K)

Z = depth into tailings from surface (m)

The first term on the right hand side represents internal heat (enthalpy) generation, while the subsequent terms express conductive, convective and latent (evaporative) enthalpy changes, respectively. As in the case of chemical and biological processes in the tailings, a monthly approach to steady state (i.e. $\delta T/\delta t = 0$) is assumed. A numerical solution for steady state conditions is given as follows:

$$Q + \frac{k \ (T_{n-1} - T_n)}{(\delta Z)^2} - \frac{k \ (T_n - T_{n+1})}{(\delta Z)^2} + \frac{F_w C_w \ (T_{n-1} - T_n)}{\delta Z} + \Delta H_{vap} \ E_w = 0 \qquad (2.3.1\text{-}2)$$

The subscripts n-1, n, and n+1 represent the successive layers and increase with depth. δZ is the distance between the layers in question. It is assumed that the temperature profile of the tailings in the absence of pyrite or other sulfidic mineral oxidation is known, thus equation (2.3.1-2) need not be solved explicitly. A difference operator "Δ" is introduced so that ΔT represents a differential temperature rise in the tailings if active sulfidic ore oxidation takes place. Equation (2.3.1-2) may be easily rewritten in terms of this temperature difference:

$$Q_{Rx} + \frac{k \ (\Delta T_{n-1} - \Delta T_n)}{(\delta Z)^2} - \frac{k \ (\Delta T_n - \Delta T_{n+1})}{(\delta Z)^2} + \frac{F_w C_w \ (\Delta T_{n-1} - \Delta T_n)}{\delta Z} = 0 \qquad (2.3.1\text{-}3)$$

Equation (2.3.1-3) is subject to the boundary condition:

$$\Delta T_1 = 0$$

where

Q_{Rx} = enthalpy generation rate due to sulfide mineral oxidation ($J.m^{-3}.s^{-1}$)

The above boundary condition is based on the assumption that the surface temperature, which is controlled by wind, radiation and other factors is not affected by sulfide mineral oxidation.

Since evaporative (i.e. latent) heat losses largely depend on surface temperature, the difference in evaporative losses was neglected.

Solution of the set of algebraic equations (one equation for each layer) was implemented in the RATAP.BMT2 program by making the thickness of zones small and assuming initially that:

$$\Delta T_{n+1} = \Delta T_{n-1} \text{ for } n \neq 1 \tag{2.3.1-4}$$

The difference, ΔT_{n+1}, was re-evaluated as the calculations progressed to the layer below the current one. Using the above equality, equation (2.3.1-3) was rewritten to yield:

$$\Delta T_n = \frac{Q_{Rx} (\delta Z)^2 + F_w C_w (\Delta T_{n-1}) (\delta Z) + 2 k (\Delta T_{n-1})}{2 k + F_w C_w (\delta Z)} \tag{2.3.1-5}$$

The calculation commenced with the second layer ($\Delta T_1 = 0$) using sulfide oxidation rates from one month previous (Q_{Rx}) for each mineral. The actual temperature was then obtained by the following:

$$T_n = T_{n,sb} + \Delta T_n \tag{2.3.1-6}$$

where

$T_{n,sb}$ = background tailings temperature in layer "n" (K)

2-18

Once the temperature is obtained, the reaction rates (Q_{Rx}) were re-evaluated in the kinetics module and the procedure was repeated until temperature convergence was obtained.

Several unforeseen problems were encountered during the running of the temperature module: the most serious problem was the slow convergence, often requiring 20 or more iterations. Temperature estimates for a particular location often fluctuated $\pm 10°C$ between each iteration. In addition, slight underprediction of temperatures from theoretical values for "steady state", long term situations was noted. These problems were largely overcome by a more efficient algorithm as described below.

Revised Temperature Algorithm for RATAP.BMT2

To develop a more efficient algorithm, equation (2.3.1-3) was rearranged as follows:

$$- \frac{k}{(\delta Z)^2} \Delta T_{n-1} + \left(\frac{2k}{(\delta Z)^2} + F_w C_w \right) \Delta T_n - \left(\frac{k}{(\delta Z)^2} + F_w C_w \right) \Delta T_{n+1} = Q_{RX} \qquad (2.3.1-7)$$

Let:

$$\frac{k}{(\delta Z)^2} = a_{n-1}$$

$$\frac{2k}{(\delta Z)^2} + F_w C_w = b_n$$

$$\frac{k}{(\delta Z)^2} + F_w C_w = c_{n+1}$$

The non-zero components (a_n, b_n, c_n) are stored as vectors and the entire temperature profile can be expressed as a tridiagonal matrix:

$$
\begin{bmatrix}
b_1 & c_1 & 0 & \cdots & & \\
a_2 & b_2 & c_2 & \cdots & & \\
& & \cdots & & & \\
& & \cdots & a_{n-1} & b_{n-1} & c_{n-1} \\
& & \cdots & 0 & a_n & b_n
\end{bmatrix}
*
\begin{bmatrix}
\Delta T_1 \\
\Delta T_2 \\
\cdots \\
\Delta T_{n-1} \\
\Delta T_n
\end{bmatrix}
=
\begin{bmatrix}
Q_{Rx(1)} \\
Q_{Rx(2)} \\
\cdots \\
Q_{Rx(n-1)} \\
Q_{Rx(n)}
\end{bmatrix}
$$

A very efficient algorithm has been developed for the tridiagonal matrix (TRIDAG) which will always succeed (Press *et al.*, 1988) for the following inequality:

$$|a|_n > |b|_n + |c|_n \tag{2.3.1-8}$$

The TRIDAG matrix solution was very successful in accelerating the convergence and resulted in "smooth" temperature profiles. Typical results are shown in Table 2.3 to Table 2.4. For comparison, the temperature profiles generated by the original RATAP.BMT2 code are shown in Table 2.5 to Table 2.6. An obvious and previously unrecognized finding is the high sensitivity of the temperature prediction to the conductivity of the tailings (KSOIL).

This sensitivity is particularly remarkable for $KSOIL < 10^6$ ($J.m^{-1}.mth^{-1}.K^{-1}$). Typical thermal conductivities may range from 1.5×10^5 to 1.5×10^6 $J.m^{-1}.mth^{-1}.K^{-1}$, hence, site dependent calibration will be important. It may be noted, that for the same KSOIL value, the TRIDAG matrix solution results in higher temperature predictions than the original RATAP.BMT2 method.

2.3.2 Sulfide Oxidation Mechanisms

The bacterial oxidation of sulfide minerals has been attributed to two mechanisms, namely, direct and indirect oxidative mechanisms. These mechanisms are by no means mutually exclusive. Their relative significance has been the subject of considerable discussion and conjecture. The direct mechanism involves an enzyme-mediated attack of the iron moiety, the sulfur moiety, or both if they occur in the same mineral to procure sulfate and/or ferric ion (Silver, 1987). In the case of chalcopyrite, for example, the stoichiometry of the reaction in acidic solutions is as follows:

2-20

Table 2.3

Temperature Profile with TRIDAG Matrix Solution, KSOIL = 10^5 J.m^{-1}.mth^{-1}. K^{-1}

						Month						
Layer	1	2	3	4	5	6	7	8	9	10	11	12
1	264.88	266.75	272.58	281.41	291.24	298.91	302.57	301.07	294.90	285.76	276.22	268.58
2	271.09	276.30	279.11	285.15	296.10	303.64	307.93	305.51	299.04	289.11	282.50	274.71
3	275.10	280.57	281.38	285.81	297.02	304.83	309.87	306.94	301.65	290.88	287.53	287.87
4	277.61	282.85	282.11	285.61	297.15	304.64	310.62	307.15	303.65	292.03	291.92	281.81
5	279.30	284.25	282.33	285.24	297.14	303.86	310.89	306.81	305.37	292.84	296.05	283.94
6	280.54	285.15	282.35	284.86	297.20	302.80	310.94	306.15	306.99	293.44	300.09	285.51
7	281.51	285.73	282.28	284.52	297.41	301.60	310.89	305.31	308.61	293.86	304.16	286.67
8	282.28	286.07	282.16	284.23	297.84	300.34	310.82	304.35	310.33	294.14	308.35	287.51
9	282.90	286.23	282.03	283.99	298.53	299.08	310.78	303.33	312.24	294.30	312.74	288.11
10	283.38	286.26	281.88	283.79	299.53	297.83	310.81	302.26	314.39	294.37	317.43	288.52
11	283.74	286.18	281.71	283.60	298.78	296.58	309.62	301.15	314.13	294.33	318.72	288.76
12	283.99	286.02	281.54	283.42	297.63	295.26	307.93	299.91	313.04	294.15	317.69	288.86
13	284.17	285.79	281.36	283.24	296.42	293.82	305.49	298.50	311.28	293.80	315.84	288.82
14	284.26	285.47	281.16	283.04	295.11	292.37	303.00	297.06	309.33	293.38	313.67	288.68
15	284.27	285.05	280.94	282.79	293.67	290.90	300.46	295.59	307.14	292.88	311.15	288.43
16	284.19	284.52	280.68	282.46	292.05	289.40	297.84	294.08	304.70	292.30	308.26	288.09
17	284.04	283.89	280.39	282.02	290.19	287.85	295.15	292.52	301.98	291.64	304.96	287.65
18	283.81	283.16	280.05	281.43	288.04	286.25	292.38	290.91	298.93	290.87	301.23	287.13
19	283.50	282.33	279.67	280.65	285.52	284.58	289.49	289.24	295.51	289.96	297.01	286.53
20	283.11	281.39	279.24	279.62	282.57	282.82	286.49	287.49	291.63	288.90	292.25	285.84

Table 2.4

Temperature Profile with TRIDAG Matrix Solution, KSOIL = 10^6 J.m^{-1}.mth^{-1}. K^{-1}

Layer	Month											
	1	2	3	4	5	6	7	8	9	10	11	12
1	264.51	265.89	271.82	280.77	290.41	298.02	301.63	300.28	294.30	285.35	275.77	268.15
2	266.39	267.40	272.21	280.29	289.56	296.95	300.88	300.12	294.71	286.83	277.88	270.33
3	268.03	268.50	272.33	279.58	288.48	295.60	299.92	299.59	294.94	287.91	279.63	272.21
4	269.49	269.45	272.41	278.90	287.38	294.21	298.89	298.89	295.04	288.73	281.13	273.86
5	270.83	270.34	272.55	278.31	286.33	292.84	297.85	298.09	295.04	289.36	282.44	275.34
6	272.07	271.20	272.75	277.83	285.37	291.54	296.81	297.25	294.95	289.84	283.57	276.68
7	273.23	272.03	273.00	277.45	284.50	290.31	295.81	296.37	294.78	290.18	284.57	277.88
8	274.32	272.84	273.31	277.16	283.74	289.17	294.86	295.48	294.56	290.40	285.44	278.96
9	275.34	273.61	273.66	276.96	283.09	288.12	293.96	294.59	294.29	290.53	286.20	279.92
10	276.30	274.36	274.04	276.84	282.40	287.15	292.85	293.71	293.86	290.57	286.71	280.79
11	277.18	275.07	274.45	276.78	281.79	286.26	291.74	292.84	293.31	290.53	287.08	281.55
12	278.00	275.76	274.88	276.78	281.27	285.46	290.68	291.99	292.72	290.41	287.35	282.22
13	278.75	276.42	275.33	276.84	280.82	284.70	289.64	291.15	292.11	290.24	287.53	282.80
14	279.44	277.04	275.78	276.93	280.43	284.02	288.66	290.34	291.49	290.02	287.64	283.30
15	280.07	277.63	276.23	277.07	280.11	283.41	287.74	289.57	290.87	289.76	287.68	283.74
16	280.64	278.18	276.68	277.23	279.84	282.86	286.88	288.83	290.24	289.47	287.67	284.10
17	281.15	278.69	277.12	277.42	279.62	282.37	286.08	288.12	289.62	289.16	287.60	284.40
18	281.60	279.17	277.56	277.62	279.44	281.95	285.32	287.45	289.01	288.82	287.49	284.64
19	282.00	279.60	277.97	277.84	279.30	281.57	284.62	286.82	288.41	288.46	287.33	284.83
20	282.35	280.00	278.37	278.06	279.18	281.24	283.96	286.22	287.82	288.09	287.13	284.97

Table 2.5

Temperature Profile with Original RATAP.BMT2 Code, KSOIL = 10^5 J.m^{-1}.mth^{-1}. K^{-1}

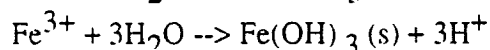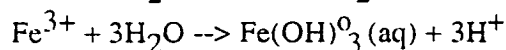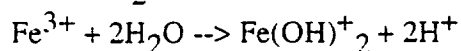| Layer	1	2	3	4	5	6	Month 7	8	9	10	11	12
1	264.47	265.80	271.74	280.69	290.31	297.92	301.53	300.19	294.24	285.28	275.72	268.10
2	266.92	268.80	273.61	281.52	290.55	298.04	301.30	301.03	294.74	287.46	278.28	270.87
3	268.97	280.57	274.31	281.24	289.95	297.17	300.46	300.90	294.93	288.84	280.24	273.06
4	270.69	271.83	274.62	280.71	289.07	296.03	299.43	300.40	294.95	289.85	281.81	274.91
5	272.19	272.92	274.88	280.21	288.13	294.83	298.32	299.74	294.86	290.60	283.13	276.53
6	273.54	273.95	275.16	279.80	287.22	293.64	297.18	299.00	294.66	291.17	284.24	277.99
7	274.79	274.93	275.49	279.47	286.38	292.52	296.05	298.21	294.38	291.59	285.19	279.29
8	275.96	275.89	275.87	279.24	285.62	291.45	294.94	297.39	294.04	291.88	285.99	280.47
9	277.05	276.80	276.28	279.10	285.59	290.49	295.38	296.57	294.33	292.06	287.41	281.51
10	278.08	277.68	276.72	279.02	285.09	289.63	294.69	295.79	294.27	292.22	288.22	282.49
11	279.03	278.51	277.19	279.02	284.61	288.83	293.88	295.02	293.94	292.25	288.76	283.34
12	279.91	279.30	277.68	279.07	284.22	288.29	293.00	294.27	293.55	292.24	289.23	284.11
13	280.73	280.07	278.18	279.18	283.90	287.64	292.23	293.51	293.05	292.14	289.55	284.76
14	281.48	280.80	278.69	279.33	283.66	287.06	291.48	292.79	292.57	291.99	289.80	285.34
15	282.18	281.50	279.21	279.53	283.47	286.56	290.79	292.09	292.07	291.80	289.98	285.84
16	282.81	282.17	279.72	279.75	283.35	286.12	290.16	291.44	291.57	291.58	290.11	286.28
17	283.39	282.79	280.22	280.00	283.28	285.75	289.63	290.85	291.09	291.34	290.19	289.69
18	283.91	283.38	280.72	280.27	283.25	285.44	289.12	290.28	290.60	291.08	290.22	287.01
19	284.37	283.94	281.20	280.56	283.27	285.18	288.66	289.74	290.13	290.80	290.24	287.30
20	284.79	284.45	281.67	280.85	283.32	284.97	288.25	289.24	289.68	290.52	290.21	287.52

Table 2.6

Temperature Profile with Original RATAP.BMT2 Code, $\text{KSOIL} = 10^6 \text{ J.m}^{-1}.\text{mth}^{-1}.\text{K}^{-1}$

							Month					
Layer	1	2	3	4	5	6	7	8	9	10	11	12
1	264.47	265.80	271.74	280.69	290.31	297.92	301.53	300.19	294.24	285.28	275.72	268.10
2	265.99	266.74	271.75	279.86	288.90	296.36	300.23	299.63	294.46	286.44	277.40	269.92
3	267.45	267.60	271.76	279.05	287.54	294.81	298.90	298.93	294.53	287.36	278.88	271.59
4	268.84	268.45	271.84	278.35	286.29	293.32	297.58	298.16	294.49	288.11	280.20	273.14
5	270.16	269.31	272.00	277.78	285.15	291.92	296.30	297.34	294.35	288.72	281.37	294.57
6	271.42	270.18	272.23	277.32	284.14	290.62	295.06	296.50	294.13	289.19	282.40	275.89
7	272.62	271.06	272.53	276.98	283.24	289.41	293.87	295.65	293.83	289.55	283.31	277.10
8	273.76	271.92	272.88	276.73	282.56	288.31	292.90	294.80	293.56	289.80	284.09	278.21
9	274.84	272.78	273.28	276.56	281.89	287.31	291.85	293.96	293.19	289.97	284.80	279.25
10	275.85	273.62	273.72	276.50	281.31	286.40	290.85	293.13	292.77	290.05	285.37	280.16
11	276.79	274.44	274.18	276.49	280.83	285.59	289.92	292.32	292.32	290.07	285.86	280.99
12	277.67	275.22	274.67	276.54	280.43	284.87	289.04	291.54	291.84	290.02	286.26	281.73
13	278.49	275.98	275.17	276.65	280.12	284.21	288.22	290.78	291.34	289.91	286.58	282.38
14	279.24	276.71	275.68	276.80	279.87	283.63	287.47	290.05	290.84	289.76	286.82	282.96
15	279.94	277.41	276.19	276.99	279.68	283.13	286.78	289.35	290.33	289.58	287.01	283.47
16	280.57	278.07	276.70	277.21	279.56	282.69	286.14	288.70	289.82	289.36	287.13	283.90
17	281.14	278.69	277.20	277.46	279.48	282.31	285.57	288.08	289.32	289.11	287.21	284.28
18	281.66	279.27	277.69	277.72	279.45	282.00	285.05	287.50	288.83	288.85	287.24	284.60
19	282.13	279.82	278.16	278.01	279.46	281.73	284.58	286.95	288.36	288.57	287.23	284.86
20	282.55	280.32	278.63	278.30	279.50	281.51	284.16	286.45	287.90	288.28	287.19	285.08

$$2FeCuS_2 + 8.5\ O_2 + 2\ H^+ \longrightarrow 2\ Fe^{3+} + 2\ Cu^{2+} + 4\ SO_4^{2-} + H_2O \qquad (2.3.2\text{-}1)$$
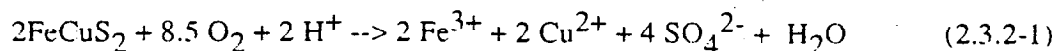
Both the oxidation of sulfide sulfur and the iron (II) moiety provide metabolic energy for the bacteria. Equation (2.3.2-1) implies net hydronium ion consumption. At pH values above 2.5, this is not observed experimentally. In fact, hydronium ions are re-generated by the hydrolysis and precipitation of dissolved iron (III) compounds:

$$Fe^{3+} + H_2O \longrightarrow Fe(OH)^{2+} + H^+ \qquad (2.3.2\text{-}2)$$
$$Fe^{3+} + 2H_2O \longrightarrow Fe(OH)^+_2 + 2H^+$$
$$Fe^{3+} + 3H_2O \longrightarrow Fe(OH)^0_3\,(aq) + 3H^+$$
$$Fe^{3+} + 3H_2O \longrightarrow Fe(OH)_3\,(s) + 3H^+$$

The indirect mechanism entails oxidation by the ferric ion in solution. The reaction products in this case are often the sulfates of the sulfide mineral and elemental sulfur. For example, pyrite (FeS_2) may be oxidized by the ferric ion in the following manner:

$$FeS_2 + Fe_2(SO_4)_3 \longrightarrow 3FeSO_4 + 2\ S^0 \qquad (2.3.2\text{-}3)$$

Equation (2.3.2-3) represents the partial oxidation of pyrite. Under certain conditions, elemental sulfur does not form in appreciable quantities and the reactions proceed to completeness (Lowson, 1982):

$$FeS_2 + 8\ H_2O + 14\ Fe^{3+} \longrightarrow 15\ Fe^{2+} + 2\ SO_4^{2-} + 16H^+ \qquad (2.3.2\text{-}4)$$
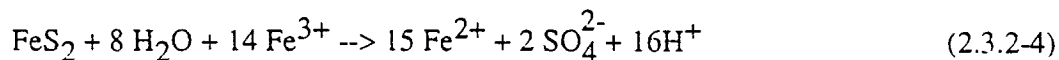
The reaction given by Equation (2.3.2-4) does not involve oxygen. Iron (III) is a very aggressive oxidizing agent for many sulfides. The rate of the redox can exceed the oxygen dependent reaction rate. Oxygen is needed, however, in the biological re-oxidation of the ferrous ion:

$$2\ Fe^{2+} + 2\ H^+ + 1/2\ O_2 \longrightarrow 2\ Fe^{3+} + H_2O \qquad (2.3.2\text{-}5)$$
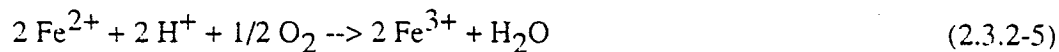
It is the re-oxidation of the ferrous ion which provides the oxidative power to maintain continual pyrite oxidation by indirect means. Equation (2.3.2-5) is often regarded as the rate limiting

process.

Bacteria are also capable of oxidizing elemental sulfur to sulfate. Several bacterial species are capable of oxidizing elemental sulfur, but *Thiobacillus ferrooxidans* and *Thiobacillus thiooxidans* are the most active under acidic conditions (Arkesteyn, 1979):

$$2\,S^0 + 3\,O_2 + 2\,H_2O \rightarrow 4\,H^+ + 2\,SO_4^{2-} \qquad (2.3.2\text{-}6)$$
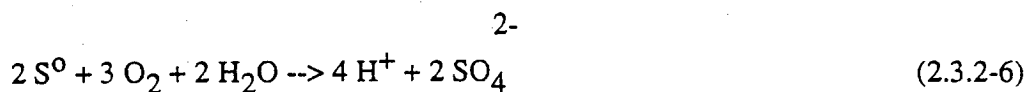
Since elemental sulfur and metal sulfide possess exceptionally low solubilities in water, surface contact is required for bacterial action. The oxidative enzymes are located in the cytoplasmic membrane on the surface of the organisms. Attachment to the mineral is often accomplished through organelles known as pili. Intimate contact of the bacteria with mineral surfaces has been shown to occur with pyrite, chalcopyrite, galena and elemental sulfur.

Several authors have attempted to find relationships between the oxidation rates and physico-chemical properties of the mineral in question. Torma and Sakaguchi (1978) reported that the rate is dependent on the solubility constant of the mineral; higher solubility results in higher oxidation rates. This suggests that the reaction rate is dependent on the availability of sulfide or hydrogen sulfide in the aqueous phase:

$$ZnS \rightarrow Zn^{2+} + S^{2-} \qquad (2.3.2\text{-}7)$$
$$S^{2-} + 2\,H^+ \rightarrow H_2S\ (aq)$$

In the past, indirect oxidation was regarded as the principal means of mineral oxidation. However, significant oxidation rates of synthetic base metal sulfides without significant quantities of iron point to direct biological oxidation as the dominant mechanism. Studies with various inhibitors have lent further support to the importance of direct bacterial participation. For example, N-ethyl maleimiole (NEM) is known to inhibit the biological oxidation of sulfide sulfur, while sodium aride inhibits enzymatic iron (II) oxidation. Observations of reaction rates obtained by the selective use of these inhibitors, either individually or in combination, have shown that the abiological and enzymatic oxidation rates of sulfur and iron are additive.

Evidence for significant indirect oxidation has been given by Arkesteyn (1979). He has demonstrated that pyrite is oxidized indirectly via bacterial oxidation of dissolved ferrous ion to

the ferric state. Bacteria and the ore were separated by a dialysis membrane. The ferric ion produced by bacterial activity diffused through the membrane and reacted with the pyrite. The overall rate of pyrite oxidation was less than in the case of direct contact with the mineral. However, in both cases, the reaction rate was greatly reduced as the pH increased to 5.0.

Unlike direct oxidation, indirect mechanisms may result in the oxidation of arsenides, silicates, selenides, and other non-sulfide minerals. Although chemical oxidation can be significant, the reaction rates are greatly increased if bacteria are present. Lacey and Lawson (1970) have estimated that the rates may be some 500,000 times greater in the presence of bacteria. Although this degree of enhancement has been observed under controlled laboratory conditions only, the importance of biological activity on mineral dissolution in natural environments has been firmly established. Five sulfides have been selected for incorporation in the model: pyrite, pyrrhotite, chalcopyrite, sphalerite and arsenopyrite.

2.3.3   Sulfide Oxidation Kinetics

Numerous investigations into the mechanisms and kinetics of bacteria-assisted sulfide oxidation have been carried out (MacDonald and Clark, 1970; Dugan and Randles, 1971; Torma *et al.*, 1972; Wong *et al.*, 1974; Hoffmann *et al.*, 1981; Tributsch and Bennett, 1981; Brown and Forshaug, 1983; Jaynes *et al.*, 1984a,b). For a heterogeneous reaction involving reactive solids such as pyrite, the specific reaction rate is normally defined (Aris, 1969) as:

$$R = -\frac{1}{A} \frac{dN_S}{dt} \qquad\qquad (2.3.3\text{-}1)$$

where

R =   the specific reaction rate $(mol.m^{-2}.mth^{-1})$

A =   the tailings particle surface area (m^2)

t =   time (mth)

N_S =   amount of sulfide (mol)

Assuming spherical symmetry, the decrease of particle size with time becomes:

$$\frac{dr}{dt} = \frac{R}{P} \qquad\qquad (2.3.3\text{-}2)$$

where

> r　=　particle radius (m)
>
> R　=　sulfide oxidation flux ($mol.m^{-2}.mth^{-1}$)
>
> P　=　molar density of the sulfide mineral ($mol.m^{-3}$)

Rearranging Equation (2.3.3-2) and solving for the sulfide content in the solid phase results in:

$$\left(\frac{N_{s,t}}{N_{s,t_0}}\right)^{1/3} = 1 - \frac{R}{P\,r_0}\,t \qquad (2.3.3\text{-}3)$$

where

> N_{s,t_0} = the initial amount of sulfide at time "t_0" (mol)

> $N_{s,t}$　=　amount of sulfide at time "t" (mol)
>
> r_0　=　initial radius of the sulfide particle (m)

Those factors which have an important influence on the rate of sulfide oxidation described by the above equations are oxygen transport and sulfide surface area (particle size).

Equation (2.3.3-3) is applicable for uniformly sized particles of known initial radius. For calculating the sulfide oxidation rate in tailings, a Paretto-type particle size frequency function is useful:

$$F(r) = A\left(\frac{r}{r_m}\right)^{\alpha} + B\left(\frac{r}{r_m}\right)^{\beta} \qquad (2.3.3\text{-}4)$$

where

> $F(r)$　=　cumulative particle size distribution function (mass fraction of particles having a radius less than "r")
>
> r_m　=　maximum radius

Using Equation (2.3.3-4) together with Equations (2.3.3-1) and (2.3.3-2), the molar mass of

2-24

pyrite at any time "t" may be estimated by the following polynomial expression:

$$\frac{N_{s,t}}{N_{s,o}} = 1 + Q_1 \left(\frac{\Sigma kt}{r_m}\right)^\alpha + Q_2 \left(\frac{\Sigma kt}{r_m}\right)^\beta + Q_3 \left(\frac{\Sigma kt}{r_m}\right)$$

$$+ Q_4 \left(\frac{\Sigma kt}{r_m}\right)^2 + Q_5 \left(\frac{\Sigma kt}{r_m}\right)^3 \qquad (2.3.3-5)$$

where

$$k = \frac{R}{P\, r_o} \qquad \text{(see Equation (2.3.3-3))}$$

The constants $a_1...a_5$ can be readily calculated from the parameters of the size distribution function. It is noteworthy that Equation (2.3.3-5) is analogous to Equation (2.3.3-3) for conditions involving variable particle size. Equation (2.3.3-5) may be easily modified for variable environmental conditions which, in turn, affects the reaction rate. In case of a variable environment, the rate constant k_t for a given time period is evaluated recursively and the term "$k_o t$" in equation 2.3.3-5 is replaced by:

$$k_o t = \sum_{n=0}^{N} k_t\, \Delta t \qquad (2.3.3-6)$$

Δt = time period (month)

The term, k_t, is usually evaluated at monthly intervals.

2.3.4 Solute Transport

Several models have been developed which predict the transfer of aqueous species in the unsaturated zone, e.g. Femwater/Femwaste (Yeh and Ward, 1979). These are based either upon a steady state or non-steady state approach.

Generally a zonal approach is used. The space is partitioned into various zones, and the law of mass balance for a dissolving substance becomes:

2-25

$$V_t \frac{dC}{dt} = q\,C_{in} - qC + r\,V_t \qquad\qquad (2.3.4\text{-}1)$$

where

V_t = porewater volume per unit area of tailings ($m^3_{water} \cdot m^{-2}_{tails}$)

C = concentration in porewater ($mol.m^{-3}$)

q = infiltration rate ($m.mth^{-1}$)

C_{in} = concentration in infiltrating rain water ($mol.m^{-3}$)

r = dissolution rate ($mol.m^{-3}.mth^{-1}$)

If the volume of water, infiltrating concentration, or dissolution rate changes substantially from timestep to timestep, then non-steady state conditions are evaluated. For this work, an approach to steady state conditions is assumed, resulting in an equation as follows:

$$C = \frac{q\,C_{in} + r\,V}{q} \qquad\qquad (2.3.4\text{-}2)$$

Equation (2.3.4-2) is known as a "mixing cell" model, since concentrations and conditions within a layer are regarded to be uniform. An alternative approach using no assumptions of uniformity gives rise to much more complex expressions. Such a model was used in UTAP (SENES, 1987). However, it may be shown that the mixing cell and the "plug flow" models give essentially identical results when a sufficient number of layers (usually more than 12) is employed.

The calculation of aqueous transportation depends upon the presence or absence of equilibrium between the solid phases and solution. Equation (2.3.4-1) assumes that equilibrium does not exist between solid phase and solution. For conditions when equilibrium does exist, the concentration of the constituent in the layer and leaving the given layer becomes:

$$C = C_{eq} \qquad\qquad (2.3.4\text{-}3)$$

where

C_{eq} = the calculated equilibrium concentration ($mol.m^{-3}$).

2-26

The mass balance above the cell affects the mass of solid phase present. It is:

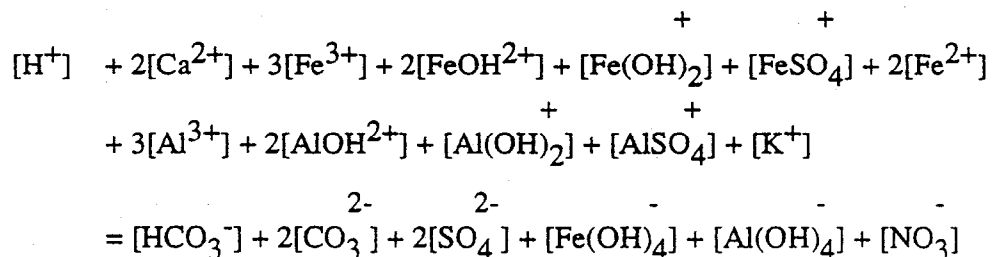$$\frac{dM}{dt} = q\,C_{in} + r\,V_t - q\,C_{eq} \qquad (2.3.4\text{-}4)$$

where

M = the mass of solid per unit volume of tailings ($mol.m^{-3}$)

For certain ions such as aluminum and iron (III), C_{eq} is a function of pH when the solid phases basaluminite and iron hydroxide occur in the tailings. This necessitates a mathematical solution of the mass balance for certain ions (e.g. K^+, Fe^{2+}), a mathematical solution of the electroneutrality equation to define C_{eq}, and solids mass balance calculations. Thus, portions of the mathematical solution for the mass balance, solids mass balance and the electroneutrality equation must be conducted simultaneously or iteratively.

2.3.5   Aqueous Speciation

The objective of the aqueous speciation module is to calculate the pH of the solution for a given composition. This calculation is based upon the electroneutrality equation which is derived from the principle of charge balance. This principle basically states that a solution must be electrically neutral and hence that the sum of positive charges in solution must equal the sum of negative charges in solution.

For ions present in leachate from the base metal tailings, the following is the electroneutrality equation:

$$[H^+] \; + 2[Ca^{2+}] + 3[Fe^{3+}] + 2[FeOH^{2+}] + [Fe(OH)_2^+] + [FeSO_4^+] + 2[Fe^{2+}]$$
$$+ \; 3[Al^{3+}] + 2[AlOH^{2+}] + [Al(OH)_2^+] + [AlSO_4^+] + [K^+]$$
$$= [HCO_3^-] + 2[CO_3^{2-}] + 2[SO_4^{2-}] + [Fe(OH)_4^-] + [Al(OH)_4^-] + [NO_3^-]$$

$$(2.3.5\text{-}1)$$

In the above equation, copper, zinc and arsenic are not included since they are assumed to be trace metals and hence have a negligible impact on the charge balance.

In Equation (2.3.5-1), the brackets [ ] represent the concentrations of these ions in solution. By balancing the concentrations of all other ions in solution, the H^+ concentration and hence the pH can be calculated directly.

However, the problem is complicated by the different procedures required to estimate the concentration of the other cations and anions. First, various ions are themselves a function of the pH. Iron (III) and aluminum hydrolyze to form various hydrolytic complexes. For example, the reaction:

$$Al^{3+} + H_2O = AlOH^{2+} + H^+ \qquad\qquad (2.3.5\text{-}2)$$

describes the hydrolysis of Al^{3+} to form $AlOH^{2+}$ and H^+. Second, various ions may be estimated from solution mass balance principles (e.g. potassium) while others (e.g. Al^{3+}, Fe^{3+}, Ca^{2+}) may be estimated from equilibrium principles. Ions are estimated from equilibrium principles if a solid phase is present, which contains the same chemical species at the identical oxidation state (valence number). If the solid phase completely dissolves, the solution mass balance is used to estimate the ion concentration. The equilibrium solution concentrations are a function of pH for various ions (e.g. aluminum and iron). For example, the solubility of iron is a function of pH according to the following precipitation reaction:

$$Fe^{3+} + 3H_2O = Fe(OH)_3(s) + 3H^+ \qquad\qquad (2.3.5\text{-}3)$$

To estimate pH, the overall electroneutrality equation must be phrased as a function of pH and appropriate total solution concentrations or solid phases, and then solved mathematically for pH. This requires that an iterative solution be used to solve the basic equations.

2.3.6   Oxygen Transport

Oxygen may be transported into porous media such as tailings by advection and/or diffusion. In the saturated zone of tailings, the diffusive transport of oxygen through the air phase is the

dominant transfer mechanism. In the capillary fringe and saturated zones of the tailings, the dominant transfer mechanism is the advection of oxygen dissolved in the infiltrating porewater.

Oxygen consumption internally in the tailings is caused mainly by sulfide mineral oxidation (i.e. by oxidative dissolution of pyrite, pyrrhotite, etc.). Small net amounts of sulfide mineral dissolution occurs in the water-filled portion of the tailings by Fe^{3+} attack upon the minerals and the reduction of Fe^{3+} to Fe^{2+}.

To account for these processes, the following assumptions are presently made in the RATAP.BMT2 model:

1)   The dominant variation in oxygen concentration occurs vertically from the air-tailings boundary downward. Any horizontal variability in oxygen concentration around the dams of the tailings pile are negligible.

2)   Sulfide mineral oxidation occurs completely in zones where oxygen is present, resulting in Fe^{3+} and SO_4^{2-} as end products (i.e. Fe^{2+} and sulfide in the sulfide minerals are fully oxidized to their highest oxidation state, Fe^{3+} and SO_4^{2-}). Thus, oxidation occurs in tailings layers containing gas-filled spaces and in the upper boundary layer of the water-filled zone where dissolved oxygen is present.

3)   Some additional sulfide mineral dissolution occurs in the anoxic zone of the water-filled layers due to the flux of Fe^{3+} into the layers from above. This has an effect upon the solution electroneutrality balance but not upon the oxygen balance.

4)   The rate of vertical transport of oxygen is much faster than the rate of sulfide mineral oxidation. Accordingly, over the time frame of variation calculated by the model (one-month), steady state conditions exist. This results in the following equations:

a)   for the gas-filled region where all air diffusion controls transport:

$$D_e \frac{d^2 C}{dx^2} - R = 0 \qquad (2.3.6\text{-}1)$$

30678 - 23 April 1990

b) for the water-filled boundary layer below the gas-filled region where advection controls transport:

$$V \frac{dC_w}{dx} - \frac{R}{n_w} = 0 \qquad (2.3.6\text{-}2)$$

where:

D_e = gas diffusion coefficient of oxygen $(m^2 . mth^{-1})$

C = gas concentration of oxygen $(mol.m^{-3})$

C_w = aqueous concentration of oxygen $(mol.m^{-3})$

x = distance in the vertical direction (m)

R = oxygen consumption rate $(mol.m^{-3}.mth^{-1})$

n_w = volumetric soil water content $(m^3_{water}.m^{-3}_{tailings})$

2-30

3.0 VALIDATION OF THE MODELLING APPROACH

3.1 Approach to Model Validation

Model validation consists of using the calibrated model to predict one or more sets of system conditions independent of the first set. If the validation is acceptable, then the model may be used, with confidence, to make predictions for purposes described in the model objectives. If the validation is not acceptable, then the model should not be used to make predictions where one requires much confidence in the predictions. If the validation is not acceptable, it may be necessary to modify the model with respect to its assumptions, or mathematical basis. Further, if the model is to be used for research purposes (to determine the most important factors in the model) or for extrapolation purposes, it must be done with care as one's confidence in the results may be fair to poor.

For model validation, several tests are possible. The first (least severe and insufficient) test is to compare the model structure (compartments and intercompartment mass flows) with the real world to determine that functional responses are reasonable and that all major factors are included. A second test involves comparing model predictions and environmental observations for one tailings pile for one time period (e.g., for a month or year) equal to or longer than the time scale of the model's objectives. A third (more severe) test involves two possibilities: (i) a comparison between model predictions and environmental observations for several tailings piles and/or (ii) a comparison between model predictions and observations from one tailings system for a time period equal to several time scales. A fourth test involves comparison between model predictions and observations for several time scales on one tailings system and for one time scale on several tailings systems. The standard used to determine the adequacy of agreement between model predictions and observations may be either qualitative (e.g., judgment of reasonableness) or quantitative (e.g., use of an appropriate statistics and lack of fit tests). To the present time, most model validation efforts have been qualitative.

Model validation was based on the comparison of model predictions for selected parameters to data collected on the Waite-Amulet tailings during the Phase 2 and Phase 3 field studies (Siwik, 1986; Siwik *et al.*, 1987; Blowes and Jambor, 1989). The database was compiled, reviewed and tested for spatial homogeneity and temporal variability. Part of the data was used to calibrate the site dependent parameter estimates. The second part of the data was used to verify the model

3-1

both in the temporal and spatial (i.e. with respect to depth) sense. Several constituents were modelled, however, only the results of porewater pH and ferrous iron predictions are included in the comparisons presented in this report. The predictability of each parameter was assessed by qualitative comparison of the simulations and field observations.

The final test involved running the model both in a deterministic and probabilistic manner. The probabilistic simulations were based on selecting parameter values from established distribution functions. The geometric mean values of the probabilistic outputs were used for comparison to the results of the deterministic runs using nominal parameter values.

3.2   Review of Previous Validation Efforts

In developing the original RATAP code, an extensive verification, calibration and validation program was carried out. Considerable use was made of data reported in the published literature and of field data collected at the Nordic uranium tailings area in Elliot Lake, Ontario. In modifying RATAP for base metal tailings applications, each of the eight component modules which comprise the RATAP.BMT1 version was modified, tested and quality assured before being integrated into the overall code to maintain the integrity of the model. Where applicable, the modules were calibrated and validated against the data base employed in the previous study. In addition, field data collected in recent years on the base metal tailings at the Waite Amulet site near Noranda-Rouyn, Quebec were employed in the model calibration and validation.

Sufficient field data at Waite Amulet were available to achieve partial calibration of the model. Predicted and measured values were found to be comparable for the solid phase pyrite and pyrrhotite contents and the gaseous phase oxygen content. The porewater pH predictions were acceptable but did not match the measured data as well as the solid and gaseous phase components. It was not practical to draw firm conclusions about the adequacy of the model predictions, however, as only a limited amount of data has been collected at Waite Amulet on certain key characteristics of the tailings. Specifically, measurements on the solid phase composition of the tailings have been made at only one location and these data showed considerable variation with depth. In addition, the results of measurements which have been made on the chemistry of the porewater in the unsaturated zone were not available at the time of this study. Also, no measurements have been made of temperature profiles in the tailings nor of the water content with depth.

3-2

To summarize, the RATAP model was successfully adapted for prediction of acid generation from base metal mine tailings. The model accounted for acid generation from the oxidation of pyrite, pyrrhotite, chalcopyrite, sphalerite and arsenopyrite; other sulfide minerals could be added in the future as required.

3.3 Extension of Validation with Waite Amulet Data

3.3.1 Characterization of the Initial Condition of the Tailings

An important aspect of the study of the geochemistry of inactive tailings impoundments is the assessment of the initial nature of the tailings solids and porewaters as they were deposited. This initial condition, which provides the basis for all future geochemical changes in the tailings, cannot be directly assessed because the mill at the Waite Amulet site closed in 1962. The initial condition of the tailings can be inferred, however, from knowledge of the milling process and from examination of tailings solids and tailings porewaters that have not been affected by sulfide oxidation.

Tailings water samples obtained from piezometers located deep in the tailings are likely to contain concentrations of dissolved constituents similar to those of the mill process waters discharged with the tailings. Porewater chemical analyses from two deep piezometers, (Siwik *et al.*, 1987) indicated that the water near the base of the impoundment is neutral in pH, and contains high concentrations of Na, Ca, SO_4 and lower concentrations of dissolved metals including Fe, Pb, Zn and Cu. This is similar to the composition expected for the mill process water (Blowes and Jambor, 1989).

An initial examination of the mineralogy in the unsaturated zone indicated that below the water table where there was minimum alteration, there was 60% pyrite and 14% pyrrhotite (Siwik *et al.*, 1988). CO_2 analysis and mineralogical studies indicated that at least trace amounts of carbonate minerals, principally calcite, are present throughout the unaltered tailings (Blowes and Jambor, 1989). Tables 3.3.-1 and 3.3-2 list some of the physical properties of Waite Amulet tailings.

TABLE 3.2-2

TAILINGS PROPERTIES AT WAITE AMULET BOREHOLES
(Blowes and Jambor, 1989)

	WA17	WA22
Depth to Water Table (m)	2.75	6
Depth to Clay (m)	11	11

TABLE 3.3-1

PHYSICAL PROPERTIES OF WAITE AMULET TAILINGS

Grain size (mm)	0.2^1
Initial oxygen activity at the tailings surface (atm)	0.21^1
Initial concentration of arsenopyrite (mass fraction)	0.005^2
Initial concentration of basaluminate (mass fraction)	0.0001^2
Initial concentration of calcite (mass fraction)	0.0003^2
Initial concentration of chalcopyrite (mass fraction)	0.003^2
Initial concentration of ferric hydroxide (mass fraction)	0.001^2
Initial concentration of gypsum (mass fraction)	0.0005^2
Initial concentration of sphalerite (mass fraction)	0.005^2
Initial concentration of sericite (mass fraction)	0.05^2
Initial concentration of pyrite (mass fraction)	0.6^3
Initial concentration of pyrrhotite (mass fraction)	0.14^3

Note

[1]   Blowes and Jambor, 1989.

[2]   SENES and Beak, 1989.

[3]   Petruk and Pinard, 1986.

3.3.2 The Sampling Program

Of the eight oxygen-concentration profiles measured at the Waite Amulet site, Blowes and Jambor (1989) considered five (WA2, WA8, WA20, WA21, WA24) unacceptable for comparison with O_2 profiles predicted using the model of Davis and Ritchie (1986). Measured on the benches of the impoundment, profiles WA20 and WA21 were subjected to compaction during dam construction. Because profiles WA2 and WA8 were saturated to within 20 cm of the tailings surface, they contained fewer than 2 data points. A clay layer at profiles WA8 and WA24, 20-40 cm thick, was placed over the tailings during the vegetation program. Of the remaining three sites (WA11, WA17 and WA22), two were chosen for validation.

WA17

At this location, two sections, totalling 300 cm, were cored. From the initial 100 cm section, 80 cm of core were recovered and divided into 5 equal sections, each assumed to be 20 cm. From this section, porewater samples are collected from 0 to 40 cm and 80 to 100 cm intervals. No water could be expressed from the core sections from 40 to 80 cm. A second core was taken from 100 to 300 cm, from which 200 cm were recovered and divided into 10 equal sections. Pore water samples were expressed from all sections of this core.

WA22

Site WA22 is located on the southern edge of the tailings where the water table is at a greater depth than at most of the other sites. A total of 600 cm of core, in three sections, was taken at this location. "The first section was cored from 0 to 100 cm, with a full 100 cm recovery. Samples were obtained from all sections squeezed except the section from 80 to 100 cm. The second core was taken between 100 and 300 cm, with full recovery, and divided into 10 equal sections. Samples were expressed from all core sections except for the two sections between 180 and 220 cm. The final core was taken from 300 cm to 600 cm, with full recovery. The last 300 cm was divided into 12 sections, each 25 cm long. Samples were obtained from each of the sections squeezed from the final core" (Blowes and Cherry, 1987).

3-4

3.3.3   Model Validation

Model validation using the Waite Amulet tailings as the test case involved running RATAP.BMT to predict pH and ferrous iron concentrations at two locations. All input parameter values were held constant between the two locations with the exception of the depth to the water table which was set equal to 2.75 metres for WA 17 and 6 metres for location WA 22. While it was recognized that there were differences in the tailings characteristics between the two locations, there was insufficient basis for changing any of the parameter values. RATAP.BMT runs were performed for one deterministic run at each location and 25 probabilistic runs at each location. The results of these runs are discussed below.

WA22

The data from this borehole was used to calibrate the model. Field data shows that "the pH in the top 1 m of core rises sharply from 3.42 in the uppermost section (Figures 3.1 and 3.2) to about 5.0 at 80 cm, then rises more slowly to a relatively constant value of about 6.4" (Blowes and Cherry, 1987). Predicted pH values agree well with measured values as indicated on Figure 3.1 for the deterministic model run and Figure 3.2 for the probabilistic model run. Both the deterministic and probabilistic model runs show more abrupt pH change with depth than is suggested by the field data.

There is good agreement between predicted and measured ferrous iron values as evidenced from the plots on Figures 3.3 and 3.4. The sharp reduction in the ferrous iron concentration between 2 and 3 metres below the tailings surface mimics the sharp rise in pH from about 4.5 to 6.5 - 7.0. This pH change contributes to the precipitation of dissolved ferrous iron as ferrous hydroxide.

The plot of the probabilistic model run includes error bars which span one standard deviation about the mean values. These error bars were calculated from the results of 25 probabilistic runs and represent the uncertainty in the predicted values due to uncertainty in the model input values, specified as distributions rather than constants. The large uncertainties predicted at a depth of 2 to 3 metres in the tailings pile are not unexpected but rather reflect the range in values which could be measured at this depth depending on the particular values selected for the input parameters.

WA 17

"The sampling program was conducted in the late fall of 1987, during a period of mixed snowfall and rainfall. The samples from WA17 were collected shortly after snowmelt had occurred, while samples from most other locations were collected through the unmelted snow cover" (Blowes and Cherry, 1987). The unusual pH values in the near surface area suggest that the water expressed from the uppermost core may reflect recently infiltrated rain or snow melt water. Below the top 100 cm the pH rises to a level between 5.0 and 6.0 (Figures 3.5 and 3.6), similar to other sites at Waite Amulet (Figure 3.1). There is reasonable agreement between predicted and measured pH values, although the lower predicted values in this case suggest that more buffering capacity may have been available at this location than was assumed. The starting mineralogical composition at WA 17 was assumed to be identical to WA 22 since location specific data were not available. A better fit of observed and predicted values could have been obtained by adjusting some of the input parameter values.

The ferrous iron concentrations plotted on Figures 3.7 and 3.8 show that the predicted values agree well with the measured values. It is noted that the measured values at WA 17 were significantly higher than measured at WA 22, and the predicted values (deterministic and probabilistic) follow the same trend.

3-6
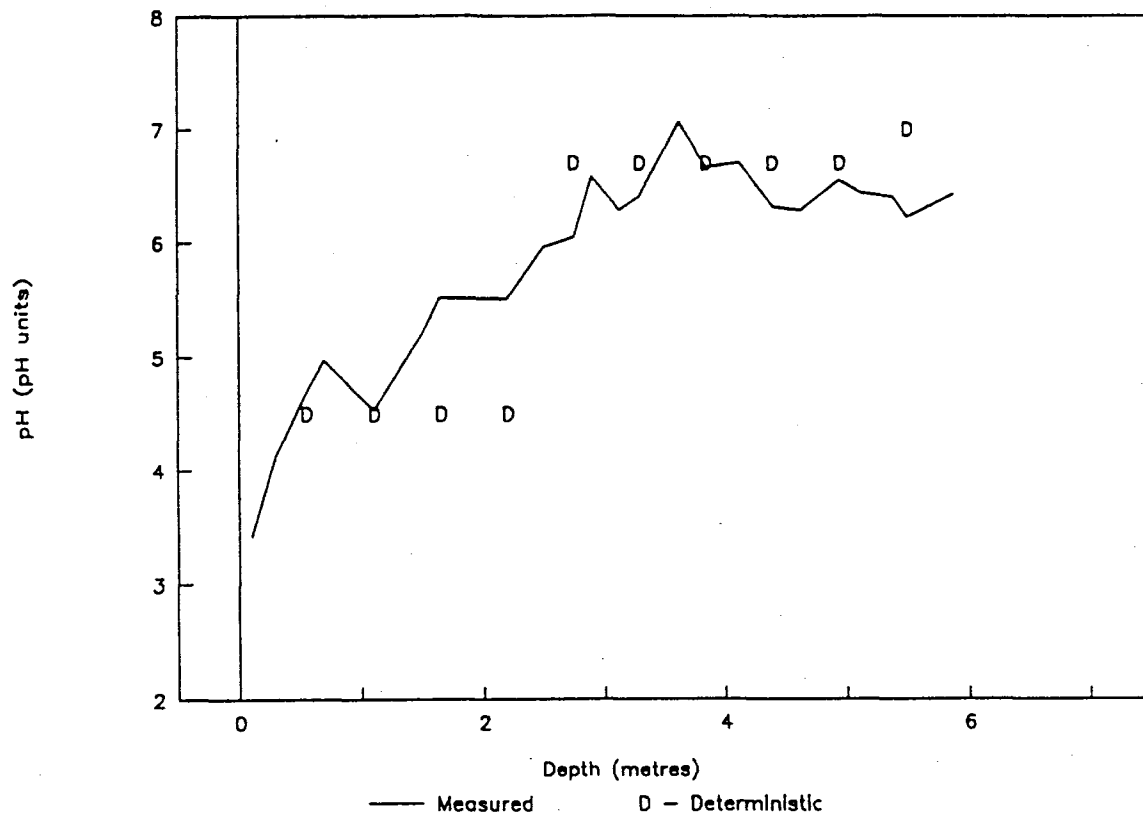
Figure 3.1   WA 22 - pH versus Depth - Deterministic Run
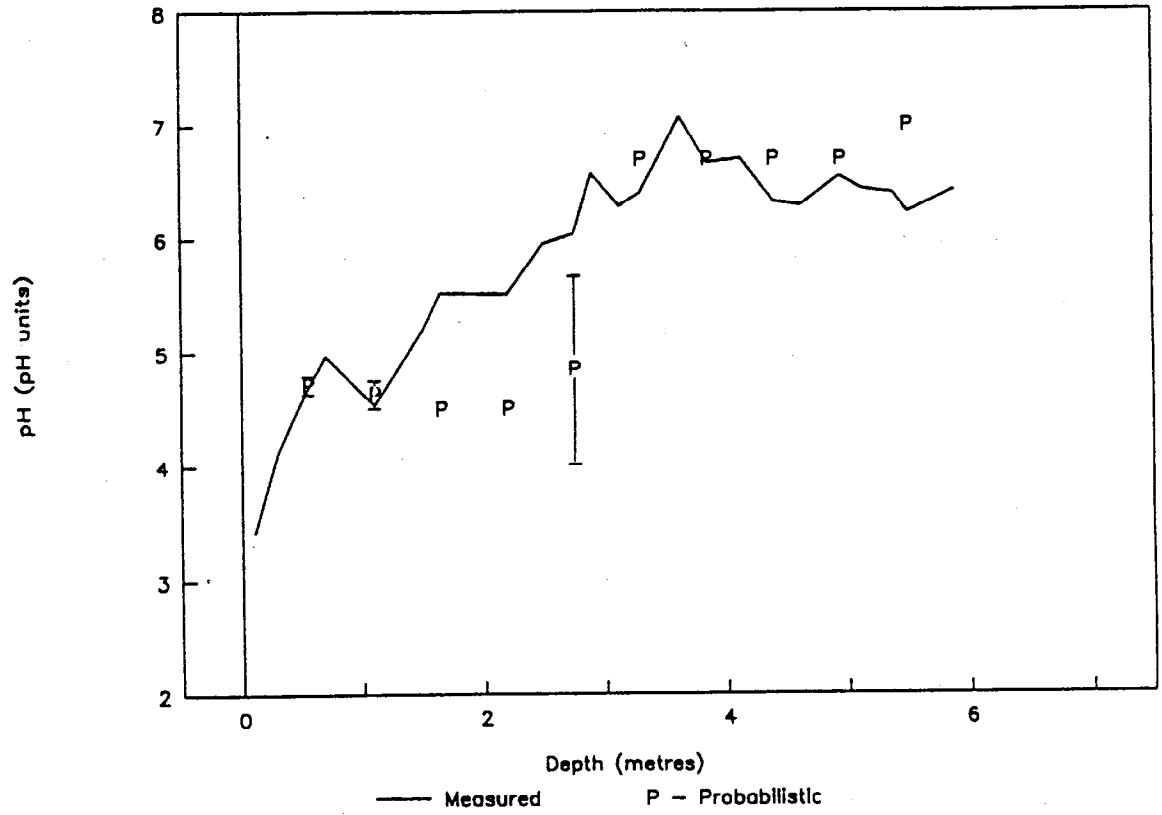
Figure 3.2   WA 22 - pH versus Depth - Probabilistic Run
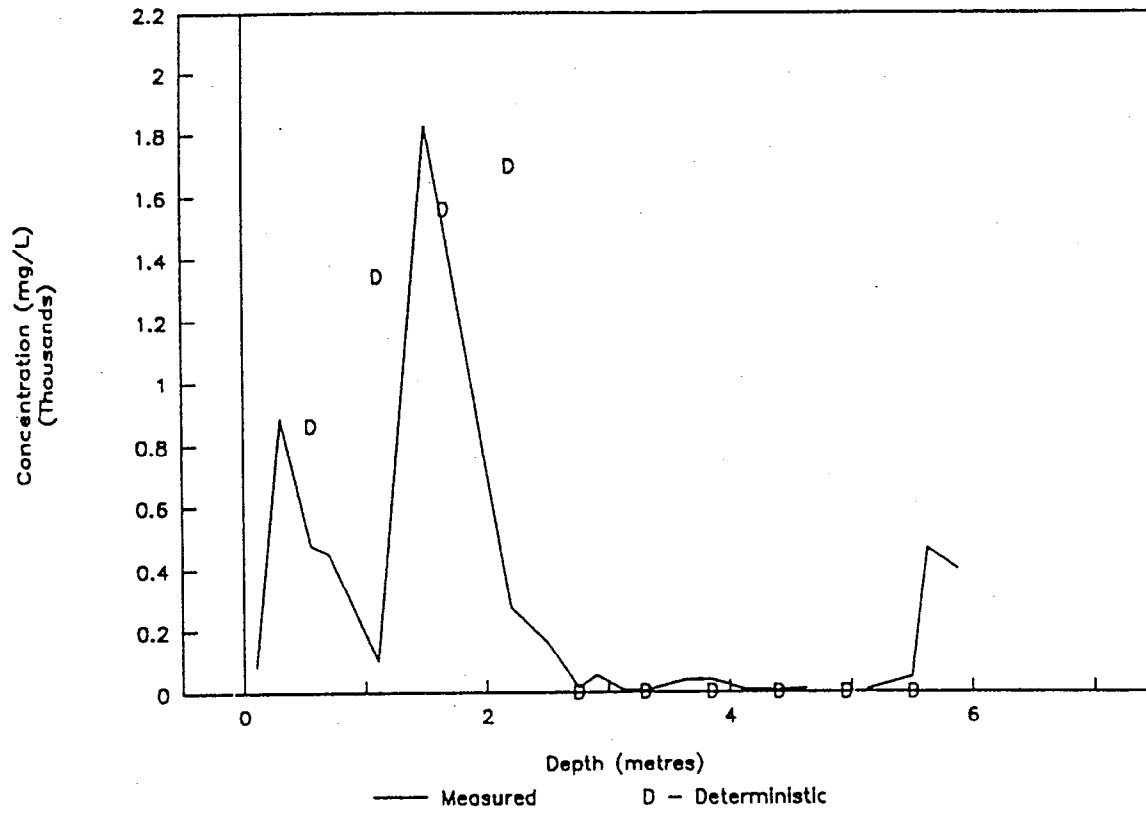
Figure 3.3   WA 22 - Ferrous Iron Concentration versus Depth - Deterministic Run
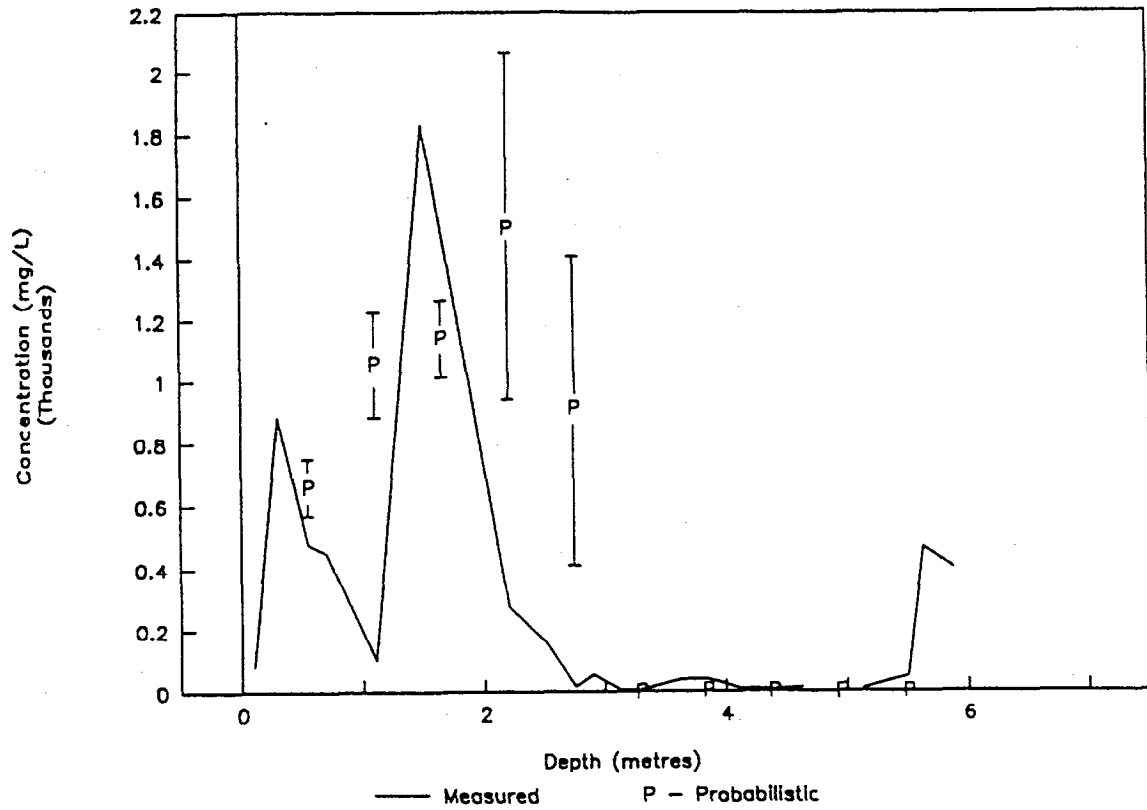
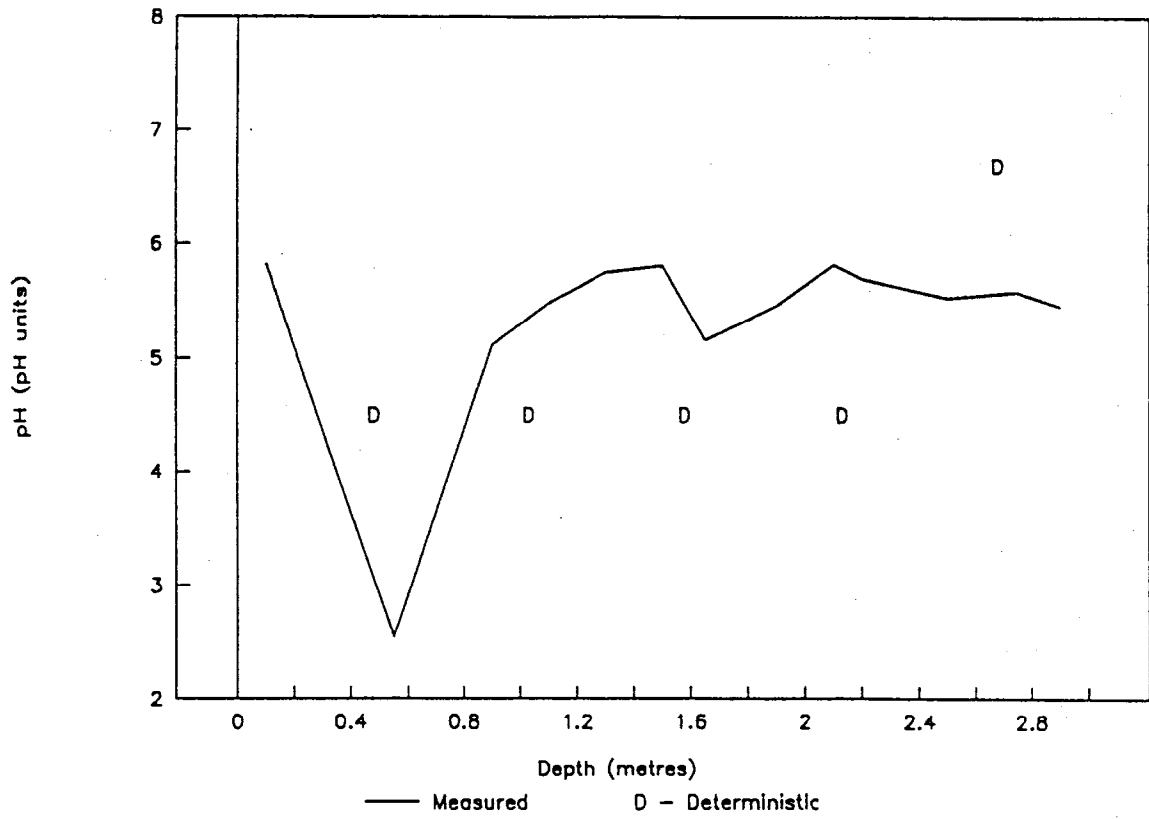Figure 3.4   WA 22 - Ferrous Iron Concentration versus Depth - Probabilistic Run

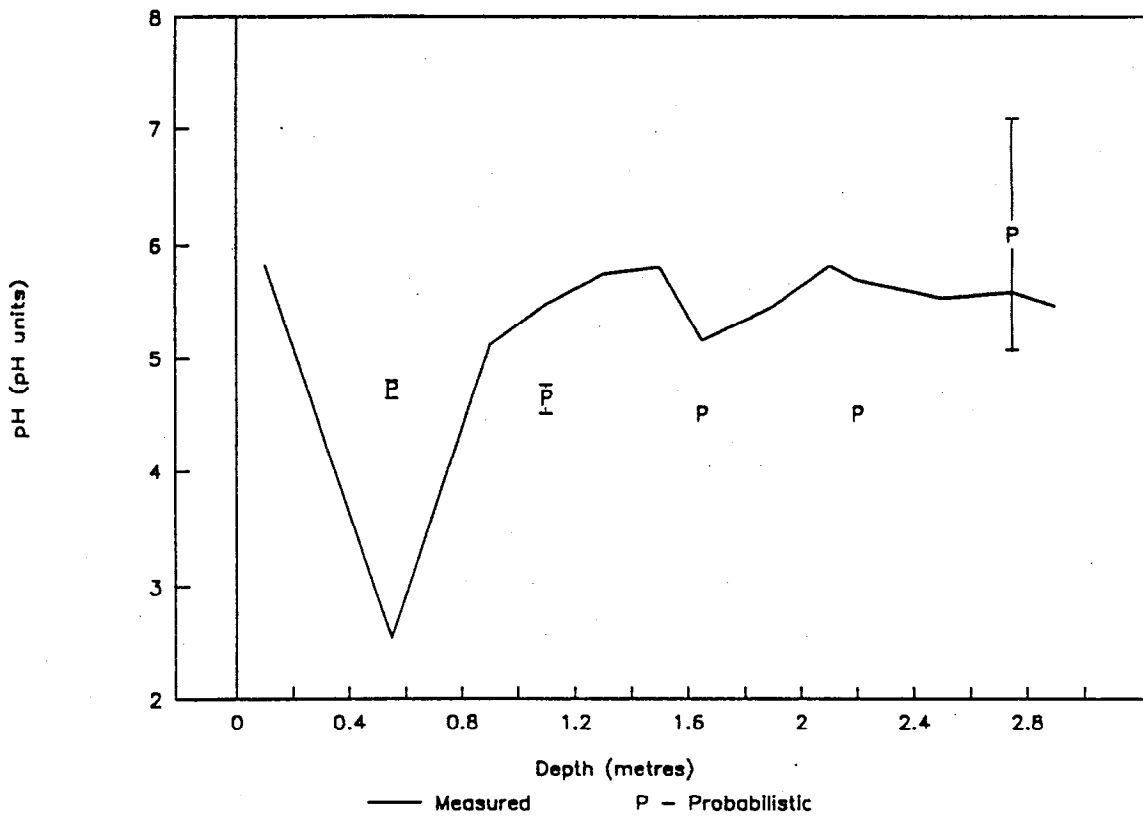Figure 3.5   WA 17 - pH versus Depth - Deterministic Run

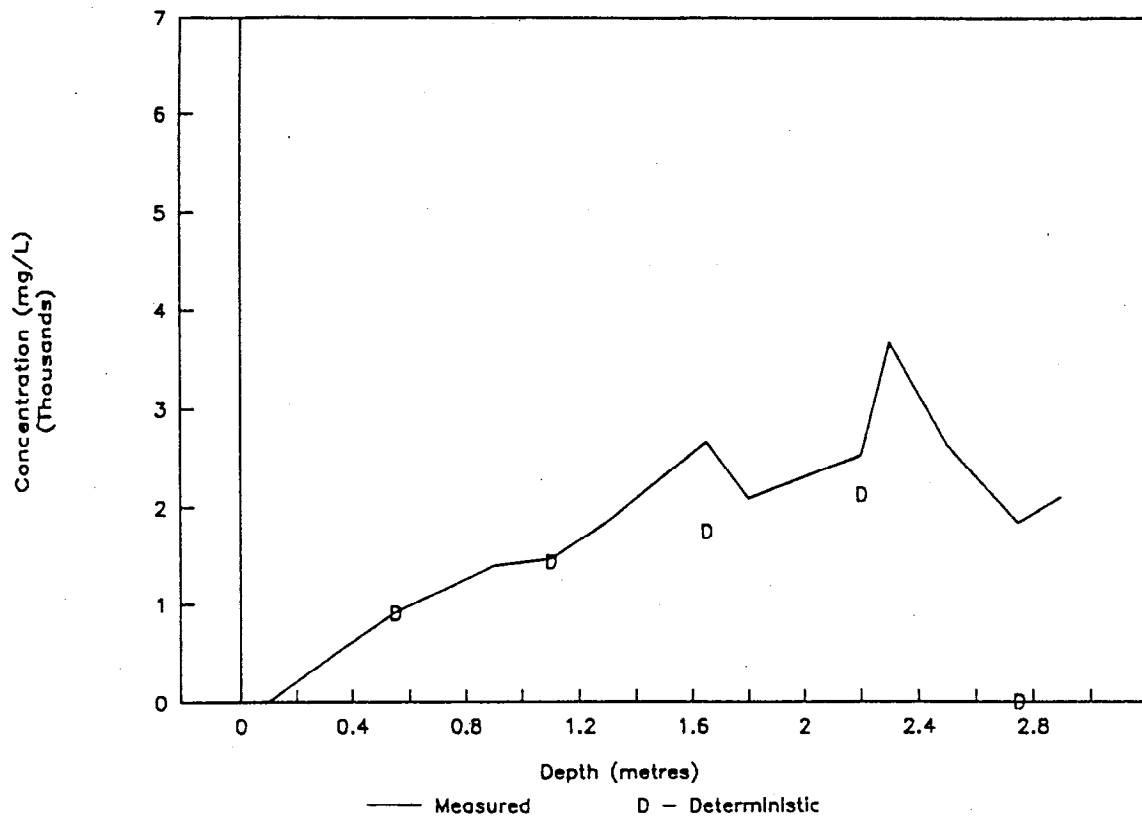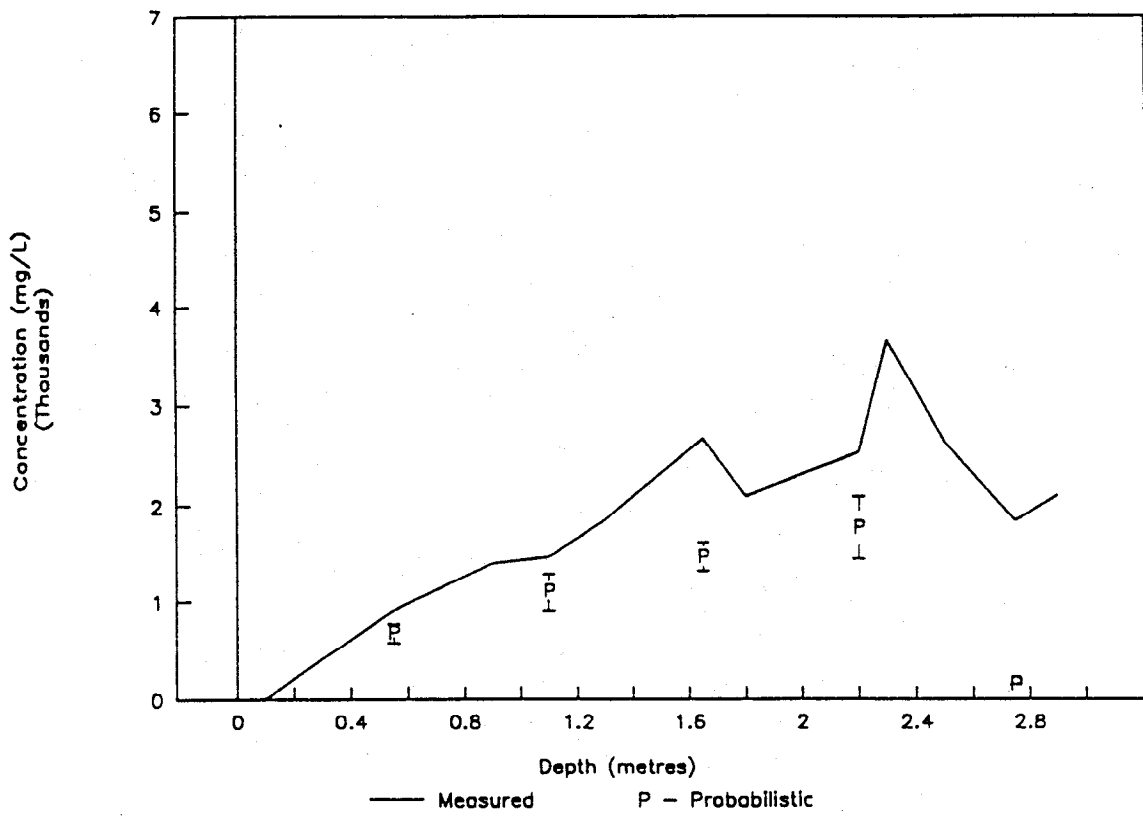Figure 3.6   WA 17 - pH versus Depth - Probabilistic Run

Figure 3.7   WA 17 - Ferrous Iron Concentration versus Depth - Deterministic Run

Figure 3.8   WA 17 - Ferrous Iron Concentration versus Depth - Probabilistic Run

4.0 CONCLUSIONS

1. RATAP.BMT addresses questions more numerous and more complex than those addressed by other acid generation models.

2. RATAP.BMT permits an evaluation of the limitations of other acid generation models.

3. RATAP.BMT permits evaluation of many additional questions which are beyond the scope of the questions evaluated by other acid generation models.

4. RATAP.BMT model structure is built around established physical and chemical principles. Empirical relationships are kept to a minimum.

5. RATAP.BMT requires a more knowledgeable user and, thus, is more difficult for a novice user to program.

6. Partial model validation was successfully performed using data collected on the Waite Amulet tailings. Further validation work is required and should preferably be undertaken on several tailings areas.

4-1

5.0 REFERENCES

Aris, R., 1969. *Elementary Chemical Reactor Analysis*. Prentice-Hall, Englewood Cliffs, N.J., p. 352.

Arkesteyn, G.J.M., 1979. *Pyrite Oxidation by Thiobacillus ferrooxidans with Special Reference to the Sulphur Moiety of the Mineral*. Atonie Van Leeuwenhoek, Vol. 45, pp. 423-425.

Bennett, J.W., Harris, J.R., Pantelis, G. and Ritchie, A.I.M., 1989. "Limitations on Pyrite Oxidation Rates in Dumps Set Up By Air Transport Mechanism". Manuscript. 11 pp with 4 figures.

Blowes, D.W. and Cherry, J.A., 1987. *Hydrogeochemical Investigations of the Unsaturated Zone of the Waite Amulet Tailings Site. Final Report*. Prepared for Noranda Research Centre. Appendix C in Siwik *et al*, 1987.

Blowes, D.W. and Jambor, J.L., 1989. *The Pore-Water Geochemistry and the Mineralogy of the Vadose Zone of Sulfide Tailings, Waite Amulet, Quebec*. Prepared for CANMET, EMR, Ottawa.

Boehm, B.W., 1984. *Verifying and Validating Software Requirements and Design Specifications*. IEEE Software Vol. 1, No. 1.

Broissia, M., 1986. *Selected Mathematical Models in Environmental Impact Assessment in Canada*. Chemical Engineering Department. University of Sherbrooke, Prepared for Canadian Environmental Assessment Research Council.

Brown, E.J. and Forshaug, J.M., 1983. *Metabolic Properties of Thiobacillus ferrooxidans Isolated from Neutral pH Mine Drainage*. Prepared for Office of Water Research and Technology, Washington, DC., PB83-208 306.

Davis, G.B. and Ritchie, A.I.M., 1986. *A Model of Oxidation in Pyritic Mine Wastes. Part 1: Equations and Approximate Solution*. Appl. Math Modelling 10, pp 314-322.

Davis, G.B., Doherty, G. and Ritchie, A.I.M., 1986. *A Model of Oxidation Pyritic Mine Wastes. Part 2: Comparison of Numerical and Approximate Solutions.* Appl. Math. Modelling 10, pp 323-329.

Davis, G.B. and Ritchie, A.I.M., 1987. *A Model of Oxidation in Pyritic Mine Wastes. Part 3: Import of Particle Size Distribution.* Appl. Math. Modelling 11, pp 417-422.

Dugan, P.R. and Randles, C.I., 1971. *The Biological System.* In: Acid Mine Drainage Formation and Abatement. By the Ohio State University Research Foundation for the U.S. Environmental Protection Agency, PB 199 835.

Harries, J.R. and Ritchie, A.IM., 1983. Water Air and Soil Pollution, 19, pp 133-170.

Hoffman, M.R., Faust, B.C., Panda, F.A., Koo, H.H., and Tsuchiya, H.M., 1981. *Kinetics of the Removal of Iron Pyrite from Coal by Microbial Catalysis.* Appl. and Env'tl. Microbiol., Vol. 42, pp. 259-271.

Jaynes, D.B., Rogowski, A.S. and Pionke, H.B., 1984a. *Acid Mine Drainage From Reclaimed Coal Strip Mines. 1. Model Description.* Water Resources Research, 20 (2), pp 233-242.

Jaynes, D.B., Poinke, H.B. and Rogowski, A.S.. 1984b. *Acid Mine Drainage From Reclaimed Coal Strip Mines. 2. Simulation Results of Model.* Water Resources Research, 29(2) pp 243-250.

Lacey, D.T. and Lawson., F., 1970. *Kinetics of the Liquid Phase Oxidation of Acid Ferrous Sulfate by the Bacterium Thiobacillus ferrooxidans.* Biotechnol. Bioeng. 12, pp. 29-50.

Lowson, R.T., 1982. *Aqueous Oxidation of Pyrite by Molecular Oxygen.* Chemical Reviews., Vol. 82, No. 5, pp. 461-497, October.

MacDonald, D.G., and Clark, R.H., 1970. *The Oxidation of Aqueous Ferrous Sulphate by Thiobaccillus ferrooxidans.* Can. J. Chem. Eng., Vol. 48, pp. 669-676.

Nicholson, R.V., Snodgrass, W.J. and Garisto, N.C., 1987. *Development of an Algorithm for the Biogeochemical Evaluation of Uranium Mill Tailings*. In Coupled Processes (Tsang ed.) pp. 339-354 McGraw Hill.

Okubo, A., 1971. Horizontal and Vertical Mixing in the Sea. "In Impingement of Man on the Oceans. (D.W. Hood Ed.). John Wiley and Sons. pp. 89.

Orlob, G.T., 1975. "Present Problems and Future Prospects of Ecological Modelling" in Ecological Modelling C.S. Rusel EA. (Washington, D.C.:" Resources for the Future Inc.) pp. 283-313.

Petruk, W. and Pinard, R.G., 1986. *Mineralogical and Image Analysis Study of Samples from Core WA20 of the Waite Amulet Tailings*. Prepared for CANMET, EMR, Ottawa, June.

Press, W.H., Flannery, B.P., Teukolsky, S.A. and Vetterling, W.T., 1988. *Numerical Recipes*. Cambridge University Press. pp. 40-41.

SENES Consultants Limited, 1984. *Report on the Assessment of the Mechanism of Bacterially-Assisted Oxidation of Pyritic Uranium Tailings*. Research Report Prepared for the National Uranium Tailings Program, CANMET, EMR, Ottawa.

SENES Consultants Limited, 1987. *Probabilistic Model Development for the Assessment of the Long-Term Effects of Uranium Mill Tailings in Canada - Phase III: Software Development and Quality Assurance Supplementary Report*. Research Report Prepared for the National Uranium Tailings Program, CANMET, EMR, Ottawa, Ontario.

SENES Consultants Limited and Beak Consultants Limited, 1986. *Estimation of the Limits of Acid Generation by Bacterially-Assisted Oxidation in Uranium Mill Tailings*. Research Report Prepared for the National Uranium Tailings Assessment Program, CANMET, EMR, Ottawa, Ontario.

SENES Consultants Limited and Beak Consultants Limited, 1987. *Reactive Acid Tailings Assessment Program (RATAP) User's Manual*. Research Report Prepared for the Canada Centre for Mineral and Energy Technology, EMR, Ottawa, Ontario.

SENES Consultants Limited and Beak Consultants Limited, 1988. *Adaptation of the Reactive Acid Tailings Assessment Program (RATAP) to Base Metal Tailings - Appendices A - I*. Research Report Prepared for the Canada Centre for Mineral and Energy Technology, EMR, Ottawa, Ontario.

SENES Consultants Limited and Beak Consultants Limited, 1989. *Reactive Acid Tailings Assessment Program (RATAP.BMT2) User's Manual*. Research Report Prepared for the Canada Centre for Mineral and Energy Technology, EMR, Ottawa, Ontario.

Silver, M., 1987. *Aquatic Plants and Bog Covers to Prevent Acid Generation - Base Metal Tailings*. In Acid Mine Drainage Seminar/Workshop Proceedings, Environment Canada, pp. 411-438.

Siwik, R.S., 1986. *Hydrogeochemical Investigation of Reactive Tailings at the Waite Amulet Tailings Site, Noranda, Quebec 1985 Program*. Final Report. Research Report Prepared for CANMET, EMR, Ottawa. July.

Siwik, R., Prairie, R., and Payant, S., 1987. *Hydrogeochemical Investigation of Reactive Tailings at Waite Amulet Tailings Sites, Noranda, Quebec Phase 2 - 1986 Program, Final Report*. Research Report Prepared for CANMET, EMR, Ottawa. July.

Siwik, R., St-Arnaud, L., Prairie, R., and Labrosse, L., 1988. *Hydrogeochemical Investigation of Reactive Tailings at Waite Amulet Tailings Site, Noranda, Quebec - Phase 3 - 1987 Program, Volume I-Report*. Research Report Prepared for CANMET, EMR, Ottawa. May.

Smyth, D.J., 1981. *Hydrogeological and Geochemical Studies Above the Water Table in an Inactive Uranium Tailings Impoundment near Elliot Lake, Ontario*. Unpublished M.Sc. Project, University of Waterloo, Waterloo, Ontario.

Thomann, R.V., 1972. *Systems Analysis and Water Quality Management*, McGraw-Hill, New York.

Torma, A.E., Walden, C.C., Duncan, D.W., Branton, R.M.R., 1972. *The Effect of Carbon Dioxide and Particle Surface Area on the Microbial Leaching of a Zinc Sulfide Concentrate.* Biotechnol. Bioeng., Vol. 15, pp. 777-786.

Torma, A.E. and Sakaguchi, H., 1978. *Relation Between the Solubility Product and The Rate of Metal Sulfide Oxidation by Thiobacillus ferrooxidans.* J. Ferm. Techn. 56, pp. 173-178.

Tributsch, H. and Bennett, J.C., 1981. *Semiconductor-Electrochemical Aspects of Bacterial Leaching. Part 2. Survey of Rate-Controlling Sulfide Properties.* J. Chem. Tech. Biotechnol., Vol. 31, pp. 627-635.

Wong, C., Scharer, J.M., and Reilly, P.M., 1974. *A Discrimination Among Microbial Iron Oxidation Mechanisms.* Can. J. Chem. Eng., Vol. 52, pp. 645-653.

Yeh, G.T., and Ward, D.S., 1979. *FEMWATER: A Finite-Element Model of Water Flow Through Saturated-Unsaturated Porous Media.* Oak Ridge National Laboratory, Report ORNL-5567.

APPENDIX A: QUALITY ASSURANCE REVIEW OF THE CODE

A.1   Overview

Mathematical models play an important and necessary role for simulating geochemical and biochemical processes in sulfidic base metal tailings. Although the individual components of these models need not be mathematically complex, the combination of the numerous components and their interaction give rise to highly non-linear model structures such as is the case with the RATAP.BMT2 model. The tracing of computer predictions is not straightforward in this case. This is particularly true if the concepts of the model have evolved through several stages. This can often result in redundant algorithms and possible coding errors that are not easily traceable.

The tracing of verification of model calculations is further complicated when models such as RATAP.BMT2 contain several iterative calculations. In the case of the RATAP.BMT2 model, the "speed" of convergence of the calculations was tested extensively and, if necessary, the iterative solution technique (Newton-Rapson vs. bisection, optimal search, etc.) was changed to give rapid convergence. However, it is believed that the current program might be further improved with respect to the iterative procedures. The computer code was also tested by analyzing the response to changes in initial conditions and parameter values.

The basic quality assurance (QA) protocol followed during each stage of development of the code is outlined below. In addition, changes made to the code as a result of the most recent QA review are documented.

A.2   QA Methodology

Two terms encountered frequently in discussions of software QA are verification and validation. Software verification can be defined as "the process of determining whether or not the products of a given phase of the software development cycle fulfill the requirements established during the previous phase" (Boehm, 1984). More succinctly, it implies constantly asking and answering the question, "Am I building the product right?" (SENES, 1987). This is probably the most useful definition, and as such, verification forms an integral part of the software QA

strategy. Software validation is when a "model with its previously defined parameters is applied in a new situation and its results are compared with field or laboratory experiments" (Broissia, 1986).

A.2.1 Verification

As an initial step during the design process, the internal structure of the model was decomposed into several modules. The logical order of the modules and the interrelationship between the modules was then established. Only after the internal structure of the model had been developed did detailed work commence on the modules.

RATAP is comprised of two basic types of modules. The computer code of the mathematical models used to simulate mine tailings and the environment are referred to as component modules, while those which provide the probabilistic framework for the simulation are referred to as control modules (SENES, 1987).

In the case of the component modules, the mathematical model details, including the species to be modelled, spatial, temporal and other considerations were translated into a series of mathematical formulae and accompanying assumptions. These formulae were then incorporated into a flowsheet illustrating the algorithm required for implementation.

In the case of control modules, an iterative flowcharting and design process was undertaken until the input/output characteristics indicated in the objectives and specifications were achieved. The control module design, review and coding preceded most of the component model coding. This allowed component models to be coded and tested within system model context and served as a test of the control modules.

Section A.3 describes the RATAP code structure while section A.4 details the line-by-line review of the RATAP source code.

A.2.2 Validation

The individual components of each module were calibrated using laboratory and/or field data whenever possible. Additionally, more comprehensive chemical speciation models were used to

confirm RATAP model predictions of individual chemical species concentrations. The comparisons are fully documented in the report by SENES and Beak (1986) and showed good agreement for all those parameters which could be tested.

Once the RATAP model development and calibration work were completed, the validity of the model predictions were tested by comparison to field data collected at the Nordic tailings site in Elliot Lake, Ontario. The tailings were deposited between 1957 and 1968 and typically contained between 3 to 8% pyrite. Several geochemical and hydrogeological investigations have been undertaken at the site in the intervening years. The data selected for comparison purposes are those reported by Smyth (1981) on two sampling stations located about 0.75 km apart and designated as T3 and T5. The tailings at location T3 are predominantly slimes and the water table at this station varies between 6 and 6.5 m below the surface. At location T5, tailings are coarse grained and the water table is at a depth of 4 to 4.5 m.

To initiate a model validation run, certain site specific information was required to characterize the tailings as they existed at the cessation of operations in 1968. Specifically, input data were required for each tailings type on the initial pyrite content, depth to water table, number of layers and thickness of each layer, tailings porosity, tailings residual water content, coefficient of moisture content and air entry value. The input values employed for all other input parameters were determined from the literature or from other field investigations in the Elliot Lake areas.

The RATAP model provides output data on a range of solid, aqueous and gaseous phase parameters. Model predictions are presented here however for only the key parameters. Figure A.2.1-1 presents a comparison of predicted and measured pyrite values at locations T3 and T5 twenty years after tailings disposal ceased. The initial pyrite content assumed for the two locations was 6% and 11%, respectively. The plots show reasonably good agreement between predicted and observed values and indicate that a substantial amount of pyrite remains above the water table at both locations.

Good agreement between predicted and measured pH values was also found at both locations (see Figure A.2.1-2). The sharp gradients in the predicted values occur when particular buffering systems are calculated to be depleted. In contract the field data suggest that the porewater may be influenced by residual solids of the buffering species which tend to smooth out the transition. The low pH values at location T5 indicate that more extensive oxidation is

occurring in the coarse tailings than in the slimes fraction at T3. This observation is expected since the coarse tailings have a lower moisture content which permits a greater oxygen flux into the tailings which, in turn, supports more complete biochemical oxidation of the sulfide minerals.

Measured and predicted total dissolved iron levels in the tailings porewater in the unsaturated zone are presented on Figure A.2.1-3. Again model predictions are seen to be in good agreement with the field data. The low iron concentrations predicted at shallow depth for location T3 occurs because pyrite is predicted to be depleted from the upper tailings horizons after twenty years of oxidation.

A.3   RATAP Code Structure

The RATAP.BMT model is divided into two parts: control modules and component modules. Control modules provide the infrastructure for the probabilistic analysis of the component modules. These modules are responsible for: 1) the random selection of values from specified input parameter distributions, 2) performing statistical analyses on user-specified input and calculated parameters and 3) managing the information transfer between modules. A detailed description of the control modules is presented in the SENES and Beak (1987) report.

Eight component modules are employed in the computer code, each performing a specific task (SENES and Beak, 1988). The modules, in order of execution, are: initial inventory, temperature, kinetics, oxygen transport, sulfide oxidation, solute transport, aqueous speciation, and trace metals. The tailings profile employed in the component modules is subdivided into distinct zones and a transition zone. In the unsaturated zone and capillary fringe, one to twenty layers are employed whereas in the saturated zone, one or two layers are used. The exact number of layers is specified in the input file.

Besides being divided into unsaturated and saturated zones, the tailings is also divided into oxidation and reduction zones. Oxidation is assumed to occur in the unsaturated zone above the hard pan. Reduction occurs below the hardpan and in the saturated zone.

Figures A.3.1 outlines the call sequence of the modules over time for the various layers. Information transferred between the modules is also identified on the figure. The first module,

A-4

executed only once, is the initial inventory module which calculates, for each layer, the initial solids composition, the monthly background tailings temperature, the tailings water content and air content. The monthly estimates are assumed to be repeated for each succeeding year.

In the temperature module, the second module, the overall tailings temperature is estimated as the background tailings temperature plus the incremental increase in temperature resulting from sulfide oxidation. The temperature module transfers the overall tailings temperature to the kinetics module, the third module, which calculates rate information (the chemical and biological oxidation rates and the oxygen consumption rate), at each time step for the various layers. The oxygen consumption rate information is then employed in the oxygen transport module, the fourth module, to calculate the oxygen profile. The oxygen module requires data on the volumetric air content of the tailings in addition to the rate information.

The next four modules, i.e. the sulfide oxidation, solute transport, aqueous speciation and trace metal modules, are all run in sequence at time t for each layer. The sulfide oxidation module imports the biological and chemical rates of oxidation for pyrite, pyrrhotite, chalcopyrite, sphalerite and arsenopyrite and the oxygen concentrations. The sulfide module then adjusts the rates to include the effect of oxygen concentration. The solute transport and aqueous speciation modules use the rates of sulfide oxidation to calculate the acid flux and pH, respectively. The solute transport and aqueous speciation routines are solved simultaneously.

The trace metal module calculates the aqueous concentration of zinc, copper and arsenic and the solid phase concentrations of copper carbonate, copper hydroxide, coprecipitated copper with iron hydroxide, copper-jarosite and sphalerite.

The pH, temperature and oxygen concentrations required for the kinetics module are estimated initially using values from the previous time step. These values are then refined seven times by being fed back into the modules and recalculating new values (see Figure A.3.1). Test calculations showed that an acceptable convergence of all parameter values was achieved in eight iterations. The values for tailings temperature, oxygen content and overall rate of oxidation fed back into the model during iterations three through eight are the geometric means of the previous two iterations.
Upon completion of these calculations, the program moves onto time period t+1 and repeats temperature through aqueous speciation modules calculations.

A.4 Line-by-Line Review of the RATAP Source Code

This task was performed by reviewing the logic of each subroutine and the logistics of calling the subroutines by the main program.

A.4.1 COMEX.FOR

The subroutine COMEX is the control module for the component modules. It is called for each time step in each trial. In RATAP.BMT2 there are eight iterations per time step. To add versatility to RATAP.BMT2, specification of the total number of iterations was changed from a constant of eight to a variable input called IGUESST. The value of IGUESST was specified in WAITED.DAT, an input file used by RATAP.BMT2.

A.4.2 INITIAL.FOR

In the INITIAL module, initial values are calculated for parameters that are dependent upon more than one input. Most of these parameters may be classified as either geochemical parameters or physical parameters.

In RATAP.BMT, lines 261 and 262 are as follows:

    261   FEOH3(I,N) = BULKD * XFEOH3/74.9
    262   ALOH3(I,N) = BULKD * XALOH3/46.0

These lines should read:

    261   FEOH3(I,N) = BULKD * XFEOH3/106.9
    262   ALOH3(I,N) = BULKD * XALOH3/78.0

because the molecular weights of $Fe(OH)_3$ and $Al(OH)_3$ are 106.9 and 78.0, respectively.

The total concentration of Ca^{2+} in the twenty-second layer is specified in line 325 of RATAP.BMT as:

    325 CAT(22,N) = 1.E-4

According to Table A.2 in Appendix A of the report, *Adaptation of the Reactive Acid Tailings Assessment Program (RATAP) to Base Metal Tailings*, line 325 should read:

    325 CAT(22,N) = 1.E-6

A-6

Similarly, the total concentration of SO_4^{2+} in the twenty-second layer is given in line 327 of RATAP.BMT as:

327 SO4T(22,N) = 1.15E-5

and should be:

327 SO4T(22,N) = 1.0E-4

A.4.3 KINETIC.FOR

In the KINETIC module, the variable R1(I,6,2) refers to the specific rate of biological reaction in $mol.m^{-2}.mth^{-1}$ in layer I. The number, 6, refers to FeS plus bacteria and the number, 2, denotes the current time step.

The variable R2(I,9,2) represents the specific rate of chemical reaction in $mol.m^{-2}, mth^{-1}$ in layer I for the present time step. The number, 9, specifies ZnS.

In RATAP.BMT, lines 178 and 181 are as follows:

178   IF(R1(I,6,2).GE.R2(I,9,2)) THEN

181   TERMX(4) = 2.0 * R1(I,6,2)

However, in line 178, R2(I,9,2) should be compared to R1(I,4,2) where 4 denotes ZnS plus bacteria. Line 178 is meant to be a comparison between the specific rate of biological reaction for ZnS and the specific rate of chemical reaction for ZnS should read as follows:

178   IF(R1(I,4,2).GE.R2(I,9,2)) THEN

Similarly, TERMX(4) represents the specific rate of oxygen depletion for sphalerite, ZnS. Thus, line 181 should be:

181   TERMX(4) = 2.0 * R1(I,4,2)

Lines 195 to 197 of KINETIC.FOR of RATAP.BMT limit RO2(I,2), the rate of oxygen depletion for layer I for the present time step, as follows:

195   IF(DX(I).LE.0.05 .AND. R02(I,2).LT.-750.)RO2(I,2) = .750.

196   IF(DX(I).GT.0.05 .AND. RO2(I,2).LT.-150.)RO2(I,2) = -.150

197   IF(DXOI).GE.0.2 .AND. RO2(I,2).LT.-75.)RO2(I,2) = -75.

RO2 is measured in $mol.m^{-3}.mth^{-1}$. These lines were deleted in RATAP.BMT2 because they impose artificial limits on RO2.

A-7

A.4.4 OXYGEN.FOR

No changes were made to OXYGEN.FOR after the line-by-line review.

A.4.5 SPECIATI.FOR

No changes were made to SPECIATI.FOR after the line-by-line review.

A.4.6 SULFIDE.FOR

Certain calculations are performed only for those layers above the capillary fringe. Line 48 in RATAP.BMT begins such a set of statements. Consequently, although it reads:

        48   IF(I.GT.LC) THEN

it should have read:

        48   IF(I.LT.LC) THEN

R1 and R2 are described in section A.4.3. In line 110 of the SULFIDE module in RATAP.BMT, R1 is compared to R2 in the same manner as in line 178 of the KINETIC module:

        110   IF(R1(I,6,2).GE.R2(I,9,2)) THEN

As is explained in section A.4.3, this should read:

        110   IF(R1(I,4,2).GE.R2(I,9,2)

Similarly, line 113 which reads:

        113   RT(I,4,2)=R1(I,6,2)

should read:

        113   RT(I,4,2)=R1(I,4,2)

Line 165 sets the previous value of TOT, an accumulator of RO2 values, to be equal to the present value of TOT. However, its placement in a DO loop causes it to accumulate too rapidly. This line was moved from the end of the DO loop.

A.4.7 TEMP.FOR

The TEMP module was rewritten after the completion of the RATAP.BMT project and was

A-8

implemented in RATAP.BMT2. A revised description of the module, *Appendix B: Temperature (Module II)*, was issued in June 1989 (SENES and Beak, 1989).

A.4.8 TRANSPOR.FOR

Ionic strength calculations yielding activity coefficients which vary with ionic strength replaced the following lines which set the activity coefficients to constant values:


```
39      F(1)=0.84
40      F(2)=0.499
41      F(3)=0.201
```

In the calculation of the ferric hydroxide concentration, FEOH3(I,3) which represents the concentration from the previous time step is used:

```
159     FEOH3(I,3)=FEOH3(I,3)-YFEOH3
```

However, FEOH3(I,2), representing the present value of the ferric hydroxide concentration, is calculated in the above expression which should read:

```
159     FEOH3(I,2)=FEOH3(I,3)-YFEOH3
```

Calculations which incorrectly refer to SULFID(1,1,2) and SULFID(1,2,2) in the following lines:

```
170     IF(SULFID(1,1,2).GT.0.)THEN
171          RATPYR=SULFID(1,1,2)/(SULFID(1,1,2)+SULFID(1,2,2))
175     SULFID(1,1,2)=SULFID(1,1,2)-REDFE3/14.*NWW(I)*DT*RATPYR
176     SULFID(1,2,2)=SULFID(1,2,2)-REDFE3/10.*NWW(I)*DT*(1.-RATPYR)
```

should refer to SULFID(I,1,2) or to SULFID(I,2,2). Also, SULFID(1,1,2) and SULFID(1,2,2) on the right hand side of the equation should be replaced by SULFID(I,1,3) and SULFID(I,2,3) where the third array subscripts, 2 and 3, indicate present and past, respectively:

```
170     IF(SULFID(I,1,2).GT.0.)THEN
171          RATPYR=SULFID(I,1,2)/(SULFID(I,1,2)+SULFID(I,2,2))
175     SULFID(I,1,2)=SULFID(I,1,3)-REDFE3/14.*NWW(I)*DT*RATPYR
176     SULFID(I,2,2)=SULFID(I,2,3)-REDFE3/10.*NWW(I)*DT*(1.-RATPYR)
```

According to solute transport theory, these lines:

```
193    XN=FE2(I,2)*SO4(I,2)-KFESO4/F(2)**2
194    XA=(XM+(XM**2-4.**XN)**0.5)/2.0
197    FESO4(I,2)=FESO4(I,2)-XA
```

should read:

```
193    XN=FE2(I,2)*SO4(I,2)-KFESO4/F(2)
194    XA=(XM+(XM**2-4.*XN)**0.5)/2.0
197    FESO4(I,2)=FESO4(I,2)+XA*NWW(I)
```

The following line which refers incorrectly to the calcium concentration for the previous time step, CA(I,3):

```
216    IF(CAEQU.GT.CA(I,3).AND.GYP(I,3).LE.0.)THEN
```

should refer to the calcium concentration for the present time step, CA(I,2):

```
216    IF(CAEQU.GT.CA(I,2).AND.GYP(I,3).LE.0.)THEN
```

```